Deflections, stresses and free vibration analysis of bi-functionally graded sandwich plates resting on Pasternak's elastic foundations via a hybrid quasi-3D theory

Pham Van Vinh

Published online: 16 Mar 2021.

Submit your article to this journal

View related articles

View Crossmark data

Taylor & Francis
Taylor & Francis Group

Check for updates

Deflections, stresses and free vibration analysis of bi-functionally graded sandwich plates resting on Pasternak's elastic foundations via a hybrid quasi-3D theory

Pham Van Vinh (ID)

Department of Solid Mechanics, Le Quy Don Technical University, Hanoi, Vietnam

ABSTRACT

The main aim of this study is to establish a hybrid quasi-3D theory for the deflections, stresses and free vibration analysis of bi-functionally graded sandwich plates resting on Pasternak's elastic foundations. In the proposed hybrid quasi-3D theory, the polynomial function is used to describe the distribution of transverse shear strains through the thickness direction while the trigonometric function is used to describe the thickness stretching effects. The bi-functionally graded sandwich plates are made of one homogeneous core and two different functionally graded face sheets. The governing equations of motion of the plates are established using Hamilton's principle and they are solved by a closed-form solution via Navier's technique. The present numerical results are compared with the published results using different higher-order and normal shear deformation theories to show the accuracy and efficiency of the proposed theory. And then the proposed theory was applied to examine the bending and free vibration behavior of the bi-functionally graded sandwich plates. A comprehensive study about the effects of some parameters such as side-to-thickness ratio, aspect ratio, skin-core-skin thicknesses, power-law index and elastic foundation parameters on the bending and free vibration behavior of the bi-functionally graded plates is carried out. The results of the deflections, stresses and frequency of the functionally graded sandwich with two different material face sheets can serve as benchmark solutions for engineering and future works.

1. Introduction

Functionally graded materials (FGMs) are widely used in the many fields of the engineering and industry (Koizumi 1997), for example, aerospace science, nuclear energy, civil engineering, etc. Therefore, many scientists have been attended to investigate the mechanical and thermal behavior of these structures via many plate theories (Swaminathan et al. 2015, Reddy 2000, Thai and Kim 2015). Inspired by the concept of FGMs, the functionally graded pattern of reinforcement has been employed for functionally graded carbon nanotube reinforced composite (FG-CNTRC) (Liew, Lei, and Zhang 2015). Some remarkable works on linear and nonlinear mechanical behavior of FG-CNTRC plates and shells have been done by Zhang and his coworkers (Zhang, Song, and Liew 2016, Zhang et al. 2016). On the other hand, the multilayer structures such as laminate composite, functionally graded sandwich plate can be used to avoid the concentration of the

stresses on the surface of the plates, beams and shells. The thermal and mechanical behavior of such structures has been investigated via numerous deformation theories. The first-order shear deformation theory (FSDT) has been used to predict the bending, free vibration and buckling of the isotropic and sandwich functionally graded plates (Altenbach and Eremeyev 2008, Nguyen, Vo, and Thai 2014, Thai et al. 2014, Mantari and Granados 2015, Nguyen et al. 2019, Gholamzadeh-Babaki and Shakouri 2019). It is obvious that FSDT is simple and fast-computing because it consists of a small number of unknown variables. However, the shear stresses do not equal to zeros at the free surfaces of the plates as natural, so it needs a shear correction factor which depends on many conditions such as materials, geometry and boundary conditions. To overcome these difficulties, many higher-order shear deformation theories (HSDTs) have been established. Reddy (1984) developed a simple higher-order theory to analyze laminated composite plates. Reddy's higher-order shear deformation theory accounts for parabolic distribution of transverse shear strains through the thickness of the plate. Pandya and Kant (1988) used the HSDT in combination with finite element method (FEM) to analyze the bending behavior of the sandwich plates. It is clear that the transverse shear stresses of the HSDT are parabolical distribution through the thickness of the plate and equal to zeros at two surfaces of the plates, so they do not need any shear correction factors. Additionally, many variations of HSDT have been developed to analyze the functionally graded sandwich (FGSW) plates (Cheshmeh et al. 2020, Vu et al.2021). Zenkour (2005a, 2005b) used sinusoidal shear deformation theory (SSDT) to investigate the bending, free vibration and buckling of FGSW plates. Many efficient refined plate theories have been developed by Meziane and his coworkers (Meziane, Abdelaziz, and Tounsi 2014, Abdelaziz et al. 2011, Bennoun, Houari, and Tounsi 2016, Meiche et al. 2011) to investigate the bending, buckling and free vibration of FGSW plates. Some other variations of HSDT have been developed to analyze isotropic and sandwich FGM plates (Nguyen et al. 2014, Van, Van, and Hoang 2020, Pham et al. 2020, Xiang and Liu 2016). The effects of porosity and thermal on the bending and buckling behavior of FGSW plate have been investigated by Daikh and Zenkour (2019), Daikh and Megueni (2018) via HSDT. It is noticeable that the HSDT is capable to analyze the moderate and thick plates, but they cannot be used to analyze very thick plates. In these cases, the quasi-3D theories are the good choices. Neves et al. (2012a, 2013) developed some quasi-3D theories incorporate with the meshless method to analyze FGSW plates. Bessaim et al. (2013) developed a new higher-order shear and normal deformation (quasi-3D) theory to analyze static and free vibration of FGSW plate. Zenkour (2013) developed a new simple quasi-3D theory with four variables of unknown to investigate the bending of FGSW plates. Natarajan and Manickam (2012) developed a family of quasi-3D theories with eleven and thirteen variables to study the bending and free vibration of FGSW plates. Afshari and Adab (2020) analyzed microplates using HSDT and quasi-3D theory. Mohseni et al. (2017) used a quasi-3D theory to analyze the bending-stretching of thick FGM micro-plates. Mantari (2015) developed a refined and generalized hybrid type quasi-3D theory shear deformation theory to analyze the bending behavior of FG plates and shells. The three-dimensional theory has been used to analyze of FGSW plate by Li, Iu, and Kou (2008). Iurlaro, Gherlone, and Sciuva (2014), Neves et al. (2012b, 2017), Dorduncu (2020) and Garg, Chalak, and Chakrabarti (2020) used zig-zag theory to analyze bending, free vibration and buckling of FGSW plates. Besides, Liu and Jeffers (2017), Pandey and Pradyumna (2015) applied layer-wise theory to analyze the mechanical behavior of FGSW plates. To consider the effects of the elastic foundation on the behavior of FGSW plates, many researchers have focused on the static and dynamic response of the FGSW plates resting on elastic foundations. Sobhy (2013) analyzed buckling and free vibration of FGSW plates resting on elastic foundations with arbitrary boundary conditions. Taibi et al. (2015) used a simple shear deformation theory to analyze thermo-mechanical behavior of FGSW plates resting on elastic foundations. Akavci (2016) studied the mechanical behavior of FGSW plates resting on elastic foundations using a quasi-3D theory. The dynamic response of FGSW plate resting on elastic
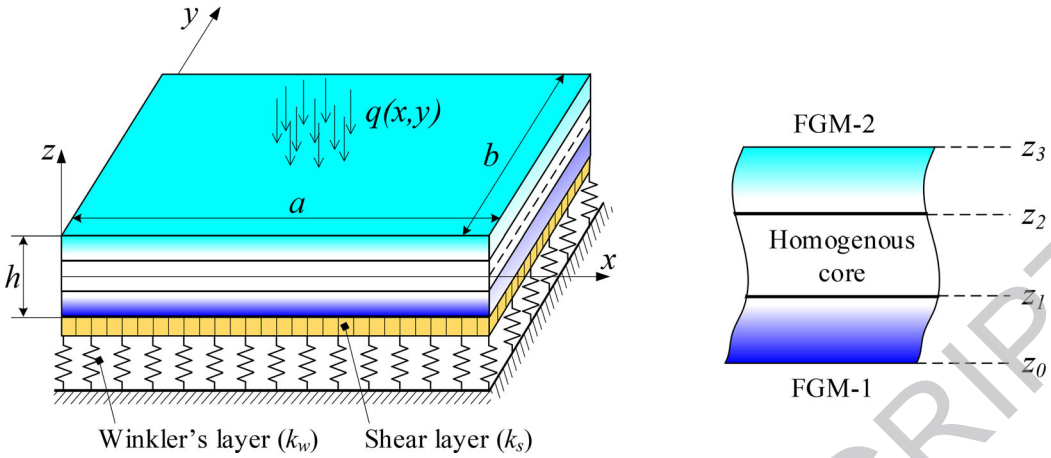
Figure 1. The model of bi-FGSW plates resting on Pasternak's elastic foundations.

foundations had been investigated by Adhikari and Singh (2019) via a quasi-3D theory. Besides, some other kinds of sandwich plates have been investigated and applied in many fields of engineering and industry, for example, piezoelectric sandwich plates, flexoelectric sandwich plates and bi-FGSW plates and so on. Arani, Zarei, and Haghparast (2018) studied vibration behavior of viscoelastic sandwich plate with magnetorheological fluid core and FG piezoelectric nanocomposite face sheets. A novel type of double-bonded sandwich microplates with nanocomposite face sheets reinforced by nanotubes has been investigated by Mohammadimehr et al. (2017). Belalia (2019) analyzed nonlinear free vibration of bi-FGSW plates using p-version of the finite element method.

It can be seen that most of the works on the behavior of FGSW plates focused on the FGSW plates with two FGM face sheets which are made of similar components. In the practical, the sandwich plate can be used in the special environment where the FGSW plate subjected to different thermal and mechanical load on its surfaces. In these cases, the bi-functionally graded sandwich (bi-FGSW) plates, which are made of one homogeneous core and two different FGM face sheets, can be used to reduce and avoid the concentration of the stresses. This study aims to analyze the static bending and free vibration of bi-FGSW plates resting on elastic foundation using a novel hybrid quasi-3D theory. Two types of bi-FGSW plates with four edges simply supported are investigated. The governing equations of motion are established via Hamilton's principle and solved via Navier's solution. A comprehensive parameter study is carried out to exhibit the behavior of two types of bi-FGSW plates with the variation of some geometry and material parameters.

2. Problem formulation

2.1. Bi-functionally graded sandwich plates resting on elastic foundations

Figure 1 shows the model of the bi-FGSW plates with the dimension of $a \times b$ and the thickness of h lies on the elastic foundations. The plate is made of one homogeneous core with the thickness of h_2 and two different functionally graded face sheets with the thicknesses of h_1 (bottom layer) and h_3 (top layer). In this study, the elastic foundation is modeled by Pasternak type elastic foundations that consists of two components which are Winkler foundation with the stiffness of k_w and shear layer with the stiffness of k_s.

The variation of the effective material properties through the thickness of the bi-FGSW plate are obtained by

Table 1. The material properties of some individual materials.

Materials	Young's modulus (GPa)	Mass density (kg/m^3)	Poisson's ratio
Al	70	2707	0.3
Ti-6Al-4V	66.2	4420	1/3
SUS304	207	8166	0.3
$(ZrO_2)_1$	151	3000	0.3
$(ZrO_2)_2$	200	5700	0.3
$(ZrO_2)_3$	117	–	1/3
Al_2O_3	380	3800	0.3
Si_3N_4	323	3170	0.3

Table 2. The construction and constituent of two types of bi-FGSW plates.

Type of bi-FGSW plates	Bottom layer	Core layer	Top layer
Type A – metal core	Si_3N_4/Ti-6Al-4V	Ti-6Al-4V	Ti-6Al-4V/Al_2O_3
Type B – ceramic core	SUS304/Al_2O_3	Al_2O_3	Al_2O_3/Ti-6Al-4V

$$\begin{cases} P(z) = P_b + (P_c - P_b)\left(\frac{z-z_0}{z_1-z_0}\right)^k & z_0 \leq z \leq z_1 \\ P(z) = P_c & z_1 < z < z_2 \\ P(z) = P_t + (P_c - P_t)\left(\frac{z-z_3}{z_2-z_3}\right)^k & z_2 \leq z \leq z_3 \end{cases} \tag{1}$$

where P_b, P_t are respectively the material properties, for example, Young's modulus, mass density and Poisson's ratio, on the bottom and top surfaces of the sandwich plates, P_c is the material properties of core layer; k is the power-law exponents of the volume fractions of FGM-1 and FGM-2 (Fig. 1), respectively. Table 1 gives the material properties of several individual materials which are used in this study. The construction and constituent of two types of bi-FGSW plates, which are used in the parameter study, are demonstrated in Table 2.

Figure 2(a, b) presents the variation of effective Young's modulus and mass density through the thickness of a $(Si_3N_4/Ti - 6Al - 4V/Al_2O_3)$ bi-FGSW plate of type A. Figure 2(c, d) provides the variation of effective Young's modulus and mass density through the thickness of a $(SUS304/Al_2O_3/Ti - 6Al - 4V)$ bi-FGSW plate of type B. According to these figures, although the skin-core-skin thicknesses are symmetric, the material properties of bi-FGSW plates are asymmetric respect to the mid-plane of the plates, it is completely different from conventional FGSW plates. When the power-law index equals zero $k = 0$, the bi-FGSW plate of type A becomes a metal plate while the bi-FGSW plate of type B becomes a ceramic one.

2.2. A Hybrid quasi-3D theory

The displacement field of the plate of new hybrid quasi-3D theory is written by

$$\begin{aligned} u(x,y,z) &= u(x,y) - z\frac{\partial w_b}{\partial x} - f(z)\frac{\partial w_s}{\partial x} \\ v(x,y,z) &= v(x,y) - z\frac{\partial w_b}{\partial y} - f(z)\frac{\partial w_s}{\partial y} \\ w(x,y,z) &= w_b(x,y) + w_s(x,y) + g(z)w_z(x,y) \end{aligned} \tag{2}$$

In which, the transverse displacement consists of three components which are the bending component w_b, the shear component w_s, and the thickness stretching component w_z. In most available quasi-3D theories, the function $g(z)$ is usually related to the first derivative of the shear deformation function $f(z)$ (Mantari 2015). According to two works of Mantari (2015), two functions $f(z)$ and $g(z)$ can be chosen freely to improve the accuracy. In this work, these functions are chosen as follows

(a) Type A $(Si_3N_4/Ti\text{-}6Al\text{-}4V/Al_2O_3)$
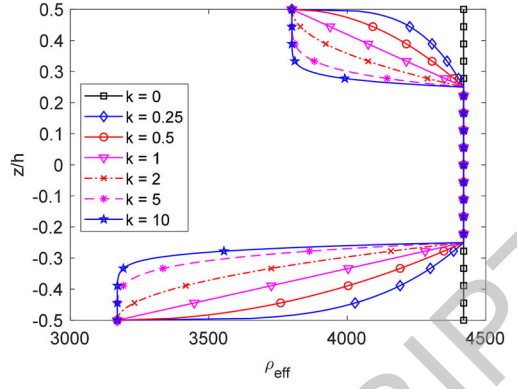
(b) Type A $(Si_3N_4/Ti\text{-}6Al\text{-}4V/Al_2O_3)$
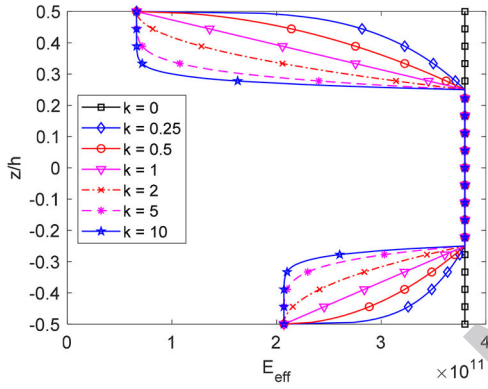
(c) Type B $(SUS304/Al_2O_3/Ti\text{-}6Al\text{-}4V)$
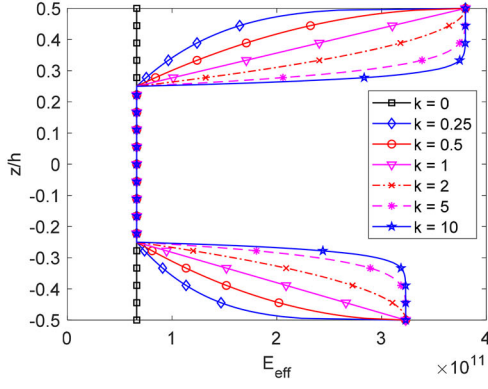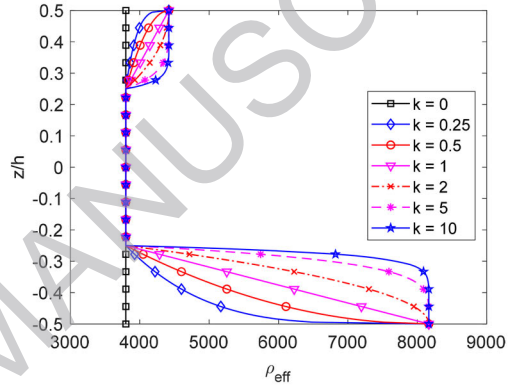
(d) Type B $(SUS304/Al_2O_3/Ti\text{-}6Al\text{-}4V)$

Figure 2. The variation of effective Young's modulus and mass density through the thickness of a (1-2-1) bi-FGSW plates.

$$f(z) = \frac{5}{3}\frac{z^3}{h^2} - \frac{1}{4}z, g(z) = \cos\left(\frac{\pi z}{h}\right) \tag{3}$$

The accuracy of the proposed theory will be proved in the next section. It also suggests that the functions $f(z)$ and $g(z)$ can be chosen spontaneously to obtain the results that are closed to the three-dimension solution. The strains fields of the plate are written as

$$\varepsilon_x = \frac{\partial u}{\partial x} - z\frac{\partial^2 w_b}{\partial x^2} - f\frac{\partial^2 w_s}{\partial x^2}$$

$$\varepsilon_y = \frac{\partial v}{\partial y} - z\frac{\partial^2 w_b}{\partial y^2} - f\frac{\partial^2 w_s}{\partial y^2}$$

$$\gamma_{xy} = \frac{\partial u}{\partial y} + \frac{\partial v}{\partial x} - 2z\frac{\partial^2 w_b}{\partial x\partial y} - 2f\frac{\partial^2 w_s}{\partial x\partial y} \tag{4}$$

$$\gamma_{xz} = r\frac{\partial w_s}{\partial x} + g\frac{\partial w_z}{\partial x}$$

$$\gamma_{yz} = r\frac{\partial w_s}{\partial y} + g\frac{\partial w_z}{\partial y}$$

$$\varepsilon_z = g'w_z$$

where $r(z) = 1 - f'(z)$. The strain field are rewritten in matrix form as

$$\left\{\begin{array}{c} \varepsilon_x \\ \varepsilon_y \\ \gamma_{xy} \end{array}\right\} = \left\{\begin{array}{c} \varepsilon_x^0 \\ \varepsilon_y^0 \\ \gamma_{xy}^0 \end{array}\right\} + z \left\{\begin{array}{c} \varepsilon_x^1 \\ \varepsilon_y^1 \\ \gamma_{xy}^1 \end{array}\right\} + f \left\{\begin{array}{c} \varepsilon_x^2 \\ \varepsilon_y^2 \\ \gamma_{xy}^2 \end{array}\right\}, \left\{\begin{array}{c} \gamma_{xz} \\ \gamma_{yz} \end{array}\right\} = r \left\{\begin{array}{c} \gamma_{xz}^0 \\ \gamma_{yz}^0 \end{array}\right\} + g \left\{\begin{array}{c} \gamma_{xz}^1 \\ \gamma_{yz}^1 \end{array}\right\}, \varepsilon_z = g' w_z \tag{5}$$

In which

$$\left\{\begin{array}{c} \varepsilon_x^0 \\ \varepsilon_y^0 \\ \gamma_{xy}^0 \end{array}\right\} = \left\{\begin{array}{c} \dfrac{\partial u}{\partial x} \\[2mm] \dfrac{\partial v}{\partial y} \\[2mm] \dfrac{\partial u}{\partial y} + \dfrac{\partial v}{\partial x} \end{array}\right\}, \left\{\begin{array}{c} \varepsilon_x^1 \\ \varepsilon_y^1 \\ \gamma_{xy}^1 \end{array}\right\} = - \left\{\begin{array}{c} \dfrac{\partial^2 w_b}{\partial x^2} \\[2mm] \dfrac{\partial^2 w_b}{\partial y^2} \\[2mm] 2\dfrac{\partial^2 w_b}{\partial x \partial y} \end{array}\right\}, \left\{\begin{array}{c} \varepsilon_x^2 \\ \varepsilon_y^2 \\ \gamma_{xy}^2 \end{array}\right\} = - \left\{\begin{array}{c} \dfrac{\partial^2 w_2}{\partial x^2} \\[2mm] \dfrac{\partial^2 w_2}{\partial y^2} \\[2mm] 2\dfrac{\partial^2 w_s}{\partial x \partial y} \end{array}\right\},$$

$$\left\{\begin{array}{c} \gamma_{xz}^0 \\ \gamma_{yz}^0 \end{array}\right\} = \left\{\begin{array}{c} \dfrac{\partial w_s}{\partial x} \\[2mm] \dfrac{\partial w_s}{\partial y} \end{array}\right\}, \left\{\begin{array}{c} \gamma_{xz}^1 \\ \gamma_{yz}^1 \end{array}\right\} = \left\{\begin{array}{c} \dfrac{\partial w_z}{\partial x} \\[2mm] \dfrac{\partial w_z}{\partial y} \end{array}\right\} \tag{6}$$

From Eq. (4) and Eq. (5), it can obvious that the plate is free of the shear strains and stresses on the top and bottom surfaces.

The constitutive equation of the sandwich plate is

$$\left\{\begin{array}{c} \sigma_x \\ \sigma_y \\ \sigma_z \\ \tau_{yz} \\ \tau_{xz} \\ \tau_{xy} \end{array}\right\}^{(n)} = \left[\begin{array}{cccccc} C_{11} & C_{12} & C_{13} & 0 & 0 & 0 \\ C_{12} & C_{22} & C_{23} & 0 & 0 & 0 \\ C_{13} & C_{23} & C_{33} & 0 & 0 & 0 \\ 0 & 0 & 0 & C_{44} & 0 & 0 \\ 0 & 0 & 0 & 0 & C_{55} & 0 \\ 0 & 0 & 0 & 0 & 0 & C_{66} \end{array}\right]^{(n)} \left\{\begin{array}{c} \varepsilon_x \\ \varepsilon_y \\ \varepsilon_z \\ \gamma_{yz} \\ \gamma_{xz} \\ \gamma_{xy} \end{array}\right\}^{(n)} \tag{7}$$

where the superscript $n = 1, 2, 3$ denotes bottom, core and top layer of the sandwich plates, respectively, and

$$C_{11} = C_{22} = C_{33} = \frac{E(z)(1 - \nu)}{(1 - 2\nu)(1 + \nu)}$$

$$C_{12} = C_{13} = C_{23} = \frac{E(z)\nu}{(1 - 2\nu)(1 + \nu)} \tag{8}$$

$$C_{44} = C_{55} = C_{66} = \frac{E(z)}{2(1 + \nu)}$$

The Hamilton's principle is employed to obtained the equations of motion

$$0 = \int_0^T (\delta \Pi - \delta V + \delta K) dt \tag{9}$$

where $\delta \Pi$ is the variation of the strain energy, δV is the variation of the work done by external forces and reaction forces of the elastic foundation and δK is the variation of the kinematic energy of the plate. The variation of the strain energy is obtained as the following expression (Akavci 2016)

$$\delta\Pi = \int_V \left(\sigma_x\delta\varepsilon_x + \sigma_y\delta\varepsilon_y + \sigma_z\delta\varepsilon_z + \tau_{xy}\delta\varepsilon_{xy} + \tau_{xz}\delta\varepsilon_{xz} + \tau_{yz}\delta\varepsilon_{yz}\right)dV \qquad (10)$$

After integrating through the thickness of the plates, one gets

$$\delta\Pi = \int_A \left[N_x\delta\varepsilon_x^0 + N_y\delta\varepsilon_y^0 + N_{xy}\delta\varepsilon_{xy}^0 + M_x\delta\varepsilon_x^1 + M_y\delta\varepsilon_y^1 + M_{xy}\delta\varepsilon_{xy}^1 + \right.$$
$$\left. + P_x\delta\varepsilon_x^2 + P_y\delta\varepsilon_y^2 + P_{xy}\delta\varepsilon_{xy}^2 + Q_y\delta\gamma_{yz}^0 + Q_x\delta\gamma_{xz}^0 + S_y\delta\gamma_{yz}^1 + S_x\delta\gamma_{xz}^1 + R_z\delta\varepsilon_z^0 \right]dA \qquad (11)$$

Inserting the Eq. (4) into Eq. (11), one gets

$$\delta\Pi = \int_A \left[N_x\frac{\partial\delta u}{\partial x} + N_y\frac{\partial\delta v}{\partial y} + N_{xy}\left(\frac{\partial\delta u}{\partial y} + \frac{\partial\delta v}{\partial x}\right) \right.$$
$$- M_x\frac{\partial^2\delta w_b}{\partial x^2} - M_y\frac{\partial^2\delta w_b}{\partial y^2} - 2M_{xy}\frac{\partial^2\delta w_b}{\partial x\partial y} +$$
$$- P_x\frac{\partial^2\delta w_s}{\partial x^2} - P_y\frac{\partial^2\delta w_s}{\partial y^2} - 2P_{xy}\frac{\partial^2\delta w_s}{\partial x\partial y} +$$
$$\left. + Q_x\frac{\partial\delta w_s}{\partial x} + Q_y\frac{\partial\delta w_s}{\partial y} + S_x\frac{\partial\delta w_z}{\partial x} + S_y\frac{\partial\delta w_z}{\partial y} + R_z\delta w_z \right]dA \qquad (12)$$

where N_i, M_i, P_i and Q_i, S_i, R_z are the stress resultants which are calculated by

$$(N_x, N_y, N_{xy}) = \sum_{n=1}^{3}\int_{z_{n-1}}^{z_n}(\sigma_x, \sigma_y, \sigma_{xy})dz$$

$$(M_x, M_y, M_{xy}) = \sum_{n=1}^{3}\int_{z_{n-1}}^{z_n}(\sigma_x, \sigma_y, \sigma_{xy})zdz$$

$$(P_x, P_y, P_{xy}) = \sum_{n=1}^{3}\int_{z_{n-1}}^{z_n}(\sigma_x, \sigma_y, \sigma_{xy})f(z)dz \qquad (13)$$

$$(Q_x, Q_y) = \sum_{n=1}^{3}\int_{z_{n-1}}^{z_n}(\sigma_{xz}, \sigma_{yz})r(z)dz$$

$$(S_x, S_y) = \sum_{n=1}^{3}\int_{z_{n-1}}^{z_n}(\sigma_{xz}, \sigma_{yz})g(z)dz$$

$$R_z = \sum_{n=1}^{3}\int_{z_{n-1}}^{z_n}\sigma_z g'(z)dz$$

After integrating through the thickness of the plates and reorder in the matrix form, one gets

$$\begin{Bmatrix} \{N\} \\ \{M\} \\ \{P\} \\ R \end{Bmatrix} = \begin{bmatrix} [A] & [B] & [E] & \{X\} \\ [B] & [D] & [F] & \{Y\} \\ [E] & [F] & [H] & \{Ys\} \\ [X] & [Y] & [Ys] & Z_{33} \end{bmatrix} \begin{Bmatrix} \{\varepsilon^0\} \\ \{k^b\} \\ \{k^s\} \\ \varepsilon_z^0 \end{Bmatrix} \qquad (14)$$

$$\left\{ \begin{array}{c} Q \\ S \end{array} \right\} = \left\{ \begin{array}{c} Q_x \\ Q_y \\ S_x \\ S_y \end{array} \right\} = \begin{bmatrix} [As] & [Bs] \\ [Bs] & [Ds] \end{bmatrix} \left\{ \begin{array}{c} \gamma^0 \\ \gamma^1 \end{array} \right\} \tag{15}$$

where

$$\left(A_{ij}, B_{ij}, E_{ij}, D_{ij}, F_{ij}, H_{ij} \right) = \sum_{n=1}^{3} \int_{z_{n-1}}^{z_n} C_{ij}\left(1, z, f, z^2, fz, f^2\right) dz \tag{16}$$

$$\left(X_{ij}, Y_{ij}, Ys_{ij}, Z_{ij} \right) = \sum_{n=1}^{3} \int_{z_{n-1}}^{z_n} C_{ij}\left(1, z, f, g'\right) g' dz \tag{17}$$

$$\left(As_{ij}, Bs_{ij}, Ds_{ij} \right) = \sum_{n=1}^{3} \int_{z_{n-1}}^{z_n} C_{ij}\left(r^2, rg, g^2\right) dz \tag{18}$$

The variation of the work done by external distributed force and reaction force of the Pasternak's elastic foundations is calculated by (Akavci 2016)

$$\delta V = -\int_A (q - R_f)\delta\left(w_b + w_s + g(0)w_z\right) dA \tag{19}$$

where R_f is the reaction force of the Pasternak's elastic foundations acting on the bottom surface of the plates, which is calculated as (Akavci 2016)

$$R_f = k_w\left(w_b + w_s + g(-h/2)w_z\right) - k_s\nabla^2\left(w_b + w_s + g(-h/2)w_z\right) \tag{20}$$

where $\nabla^2 = \frac{\partial^2}{\partial x^2} + \frac{\partial^2}{\partial y^2}$.

The variation of the kinematic energy of the plate is expressed as (Akavci 2016)

$$\delta K = \int_V \left(\dot{u}\delta\dot{u} + \dot{v}\delta\dot{v} + \dot{w}\delta\dot{w}\right)\rho(z) dV \tag{21}$$

Substituting Eq. (2) into Eq. (21), one gets

$$\begin{aligned} \delta K = \int_V &\left[\left(\dot{u}\delta\dot{u} + \dot{v}\delta\dot{v} + (\dot{w}_b + \dot{w}_s)(\delta\dot{w}_b + \delta\dot{w}_s)\right) + \right. \\ &-z\left(\dot{u}\frac{\partial\delta\dot{w}_b}{\partial x} + \frac{\partial\dot{w}_b}{\partial x}\delta\dot{u} + \dot{v}\frac{\partial\delta\dot{w}_b}{\partial y} + \frac{\partial\dot{w}_b}{\partial y}\delta\dot{v}\right) + \\ &-f\left(\dot{u}\frac{\partial\delta\dot{w}_s}{\partial x} + \frac{\partial\dot{w}_s}{\partial x}\delta\dot{u} + \dot{v}\frac{\partial\delta\dot{w}_s}{\partial y} + \frac{\partial\dot{w}_s}{\partial y}\delta\dot{v}\right) + \\ &+z^2\left(\frac{\partial\dot{w}_b}{\partial x}\frac{\partial\delta\dot{w}_b}{\partial x} + \frac{\partial\dot{w}_b}{\partial y}\frac{\partial\delta\dot{w}_b}{\partial y}\right) + \\ &+fz\left(\frac{\partial\dot{w}_b}{\partial x}\frac{\partial\delta\dot{w}_s}{\partial x} + \frac{\partial\dot{w}_s}{\partial x}\frac{\partial\delta\dot{w}_b}{\partial x} + \frac{\partial\dot{w}_b}{\partial y}\frac{\partial\delta\dot{w}_s}{\partial y} + \frac{\partial\dot{w}_s}{\partial y}\frac{\partial\delta\dot{w}_b}{\partial y}\right) + \\ &+f^2\left(\frac{\partial\dot{w}_s}{\partial x}\frac{\partial\delta\dot{w}_s}{\partial x} + \frac{\partial\dot{w}_s}{\partial y}\frac{\partial\delta\dot{w}_s}{\partial y}\right) + \\ &+g\left((\dot{w}_b + \dot{w}_s)\delta\dot{w}_z + \dot{w}_z(\delta\dot{w}_b + \delta\dot{w}_s)\right) + \\ &\left. +g^2\dot{w}_z\delta\dot{w}_z\right]\rho(z) dV \end{aligned} \tag{22}$$

After integrating through the thickness of the plates, one gets

$$\delta K = \int_A \Bigg[I_0(\dot{u}\delta\dot{u} + \dot{v}\delta\dot{v} + (\dot{w}_b + \dot{w}_s)(\delta\dot{w}_b + \delta\dot{w}_s)) + I_1\left(\dot{u}\frac{\partial\delta\dot{w}_b}{\partial x} + \frac{\partial\dot{w}_b}{\partial x}\delta\dot{u} + \dot{v}\frac{\partial\delta\dot{w}_b}{\partial y} + \frac{\partial\dot{w}_b}{\partial y}\delta\dot{v}\right)$$

$$+ I_2\left(\dot{u}\frac{\partial\delta\dot{w}_s}{\partial x} + \frac{\partial\dot{w}_s}{\partial x}\delta\dot{u} + \dot{v}\frac{\partial\delta\dot{w}_s}{\partial y} + \frac{\partial\dot{w}_s}{\partial y}\delta\dot{v}\right) + I_3\left(\frac{\partial\dot{w}_b}{\partial x}\frac{\partial\delta\dot{w}_b}{\partial x} + \frac{\partial\dot{w}_b}{\partial y}\frac{\partial\delta\dot{w}_b}{\partial y}\right)$$

$$+ I_4\left(\frac{\partial\dot{w}_b}{\partial x}\frac{\partial\delta\dot{w}_s}{\partial x} + \frac{\partial\dot{w}_s}{\partial x}\frac{\partial\delta\dot{w}_b}{\partial x} + \frac{\partial\dot{w}_b}{\partial y}\frac{\partial\delta\dot{w}_s}{\partial y} + \frac{\partial\dot{w}_s}{\partial y}\frac{\partial\delta\dot{w}_b}{\partial y}\right) + I_5\left(\frac{\partial\dot{w}_s}{\partial x}\frac{\partial\delta\dot{w}_s}{\partial x} + \frac{\partial\dot{w}_s}{\partial y}\frac{\partial\delta\dot{w}_s}{\partial y}\right)$$

$$+ I_6((\dot{w}_b + \dot{w}_s)\delta\dot{w}_z + \dot{w}_z(\delta\dot{w}_b + \delta\dot{w}_s)) + I_7\dot{w}_z\delta\dot{w}_z\Bigg]dA$$

(23)

where

$$(I_0, I_1, I_2, I_3, I_4, I_5, I_6, I_7) = \sum_{n=1}^{3} \int_{z_{n-1}}^{z_n} \rho(z)\big(1, -z, -f, z^2, fz, f^2, g, g^2\big)dz \tag{24}$$

Substituting Eqs. (12), (19) and Eq. (23) into Eq. (9) and integrating by parts, the equilibrium equations of the plates are obtained as following formulae

$$\delta u: -\frac{\partial N_x}{\partial x} - \frac{\partial N_{xy}}{\partial y} = -I_0\ddot{u} - I_1\frac{\partial\ddot{w}_b}{\partial x} - I_2\frac{\partial\ddot{w}_s}{\partial x},$$

$$\delta v: -\frac{\partial N_y}{\partial y} - \frac{\partial N_{xy}}{\partial x} = -I_0\ddot{v} - I_1\frac{\partial\ddot{w}_b}{\partial y} - I_2\frac{\partial\ddot{w}_s}{\partial y},$$

$$\delta w_b: -\frac{\partial^2 M_x}{\partial x^2} - 2\frac{\partial^2 M_{xy}}{\partial x\partial y} - \frac{\partial^2 M_y}{\partial y^2} = q - k_w(w_b + w_s) + k_s\nabla^2(w_b + w_s)$$

$$-I_0(\ddot{w}_b + \ddot{w}_s) + I_1\left(\frac{\partial\ddot{u}}{\partial x} + \frac{\partial\ddot{v}}{\partial y}\right) + I_3\left(\frac{\partial\ddot{w}_b}{\partial x^2} + \frac{\partial\ddot{w}_b}{\partial y^2}\right) + I_4\left(\frac{\partial\ddot{w}_s}{\partial x^2} + \frac{\partial\ddot{w}_s}{\partial y^2}\right) - I_6\ddot{w}_z,$$

$$\delta w_s: -\frac{\partial^2 P_x}{\partial x^2} - 2\frac{\partial^2 P_{xy}}{\partial x\partial y} - \frac{\partial^2 P_y}{\partial y^2} - \frac{\partial Q_x}{\partial x} - \frac{\partial Q_y}{\partial y} = q - k_w(w_b + w_s) + k_s\nabla^2(w_b + w_s)$$

$$-I_0(\ddot{w}_b + \ddot{w}_s) + I_2\left(\frac{\partial\ddot{u}}{\partial x} + \frac{\partial\ddot{v}}{\partial y}\right) + I_4\left(\frac{\partial\ddot{w}_b}{\partial x^2} + \frac{\partial\ddot{w}_b}{\partial y^2}\right) + I_5\left(\frac{\partial\ddot{w}_s}{\partial x^2} + \frac{\partial\ddot{w}_s}{\partial y^2}\right) - I_6\ddot{w}_z,$$

$$\delta w_z: -\frac{\partial S_x}{\partial x} - \frac{\partial S_y}{\partial y} + R_z = q - I_6(\ddot{w}_b + \ddot{w}_s) - I_7\ddot{w}_z \tag{25}$$

It is noticed that $g(h/2) = g(-h/2) = 0$.

2.3. Navier's solution

In this study, a fully simple supported FGM plate subjected to a distributed transverse load is considered. The Navier's solution technique is employed to solve the equations of motion, the unknown displacement functions of the plates are assumed as following formulae (Bennoun, Houari, and Tounsi 2016)

$$u(x, y, t) = \sum_{\alpha=1}^{\infty} \sum_{\beta=1}^{\infty} U_{\alpha\beta} \cos \eta_\alpha x \sin \vartheta_\beta y. e^{i\omega t}$$

$$v(x, y, t) = \sum_{\alpha=1}^{\infty} \sum_{\beta=1}^{\infty} V_{\alpha\beta} \sin \eta_\alpha x \cos \vartheta_\beta y. e^{i\omega t}$$

$$w_b(x, y, t) = \sum_{\alpha=1}^{\infty} \sum_{\beta=1}^{\infty} Wb_{\alpha\beta} \sin \eta_\alpha x \sin \vartheta_\beta y. e^{i\omega t} \tag{26}$$

$$w_s(x, y, t) = \sum_{\alpha=1}^{\infty} \sum_{\beta=1}^{\infty} Ws_{\alpha\beta} \sin \eta_\alpha x \sin \vartheta_\beta y. e^{i\omega t}$$

$$w_z(x, y, t) = \sum_{\alpha=1}^{\infty} \sum_{\beta=1}^{\infty} Wz_{\alpha\beta} \sin \eta_\alpha x \sin \vartheta_\beta y. e^{i\omega t}$$

where $\eta_\alpha = \alpha\pi/a$ and $\vartheta_\beta = \beta\pi/b$.

The distributed load is expanded as follows

$$q(x, y) = \sum_{\alpha=1}^{\infty} \sum_{\beta=1}^{\infty} \Omega_{\alpha\beta} \sin \eta_\alpha x \sin \vartheta_\beta y \tag{27}$$

where $\Omega_{\alpha\beta}$ depends on the load types. In the case of double sinusoidal load, $\Omega_{\alpha\beta}$ are calculated as follows

$$\begin{cases} \Omega_{\alpha\beta} = q_0 & \alpha = \beta = 1 \\ \Omega_{\alpha\beta} = 0 & \alpha \neq 1, \beta \neq 1 \end{cases} \tag{28}$$

Substituting Eq. (26) and Eq. (27) into Eq. (25), one gets

$$\left(\begin{bmatrix} k_{11} & k_{12} & k_{13} & k_{14} & k_{15} \\ & k_{22} & k_{23} & k_{24} & k_{25} \\ & & k_{33} & k_{34} & k_{35} \\ sys & & & k_{44} & k_{45} \\ & & & & k_{55} \end{bmatrix} - \omega^2 \begin{bmatrix} m_{11} & m_{12} & m_{13} & m_{14} & m_{15} \\ & m_{22} & m_{23} & m_{24} & m_{25} \\ & & m_{33} & m_{34} & m_{35} \\ sys & & & m_{44} & m_{45} \\ & & & & m_{55} \end{bmatrix} \right) \begin{Bmatrix} U_{\alpha\beta} \\ V_{\alpha\beta} \\ Wb_{\alpha\beta} \\ Ws_{\alpha\beta} \\ Wz_{\alpha\beta} \end{Bmatrix} = \begin{Bmatrix} 0 \\ 0 \\ \Omega_{\alpha\beta} \\ \Omega_{\alpha\beta} \\ \Omega_{\alpha\beta} \end{Bmatrix} \tag{29}$$

where $k_{ij}, m_{ij}, i, j = \overline{1,5}$ are calculated as following formulae

$$k_{11} = A_{11}\eta^2 + A_{66}\vartheta^2, k_{12} = (A_{12} + A_{66})\vartheta\eta, k_{13} = -B_{11}\eta^3 - (B_{12} + 2B_{66})\vartheta^2\eta$$

$$k_{14} = -E_{11}\eta^3 - (E_{12} + 2E_{66})\vartheta^2\eta, k_{15} = -X_{13}\eta, k_{22} = A_{22}\vartheta^2 + A_{66}\eta^2$$

$$k_{23} = -B_{22}\vartheta^3 - (B_{12} + 2B_{66})\eta^2\vartheta, k_{24} = -E_{22}\vartheta^3 - (E_{12} + 2E_{66})\eta^2\vartheta$$

$$k_{25} = -X_{23}\vartheta, k_{33} = D_{11}\eta^4 + \left((4D_{66} + 2D_{12})\vartheta^2 + k_s\right)\eta^2 + D_{22}\vartheta^4 + \vartheta^2 k_s + k_w \tag{30}$$

$$k_{34} = F_{11}\eta^4 + \left(2(F_{12} + 2F_{66})\vartheta^2 + k_s\right)\eta^2 + F_{22}\vartheta^4 + \vartheta^2 k_s + k_w, k_{35} = Y_{13}\eta^2 + Y_{23}\vartheta^2$$

$$k_{44} = \eta^4 H_{11} + \left((2H_{12} + 4H_{66})\vartheta^2 + k_s + As_{55}\right)\eta^2 + H_{22}\vartheta^4 + (k_s + As_{44})\vartheta^2 + k_w$$

$$k_{45} = (Ys_{13} + Bs_{55})\eta^2 + (Ys_{23} + Bs_{44})\vartheta^2, k_{55} = Ds_{44}\vartheta^2 + Ds_{55}\eta^2 + Z_{33}$$

$$m_{11} = I_0, m_{12} = 0, m_{13} = I_1\eta, m_{14} = I_2\eta, m_{15} = 0,$$

$$m_{22} = I_0, m_{23} = I_1\vartheta, m_{24} = I_2\vartheta, m_{25} = 0$$

$$m_{33} = (\eta^2 + \vartheta^2)I_3 + I_0, m_{34} = (\eta^2 + \vartheta^2)I_4 + I_0, m_{35} = I_6 \tag{31}$$

$$m_{44} = (\eta^2 + \vartheta^2)I_5 + I_0, m_{45} = I_6, m_{55} = I_7$$

Table 3. The comparison of the dimensionless center deflection and axial normal stress of square FGSW plates without elastic foundation.

k	Theory	ε_z	$\bar{w}$				$\bar{\sigma}_x$			
			2-1-2	1-1-1	2-2-1	1-2-1	2-1-2	1-1-1	2-2-1	1-2-1
0	Thai et al. 2014 (FSDT)	$= 0$	0.1961	0.1961	0.1961	0.1961	1.9758	1.9758	1.9758	1.9758
	Zenkour 2005a (FSDT)	$= 0$	0.19607	0.19607	0.19607	0.19607	1.97576	1.97576	1.97576	1.97576
	Zenkour 2005a (SSDT)	$= 0$	0.19605	0.19605	0.19605	0.19605	2.05452	2.05452	2.05452	2.05452
	Neves et al. 2012b	$= 0$	0.19610	0.19610	0.19610	0.19610	1.99470	1.99470	1.99460	1.99460
	Neves et al. 2012b	$\neq 0$	0.19490	0.19490	0.19490	0.19490	2.00660	2.00660	2.00650	2.00640
	Bessaim et al. 2013	$\neq 0$	0.19486	0.19486	0.19486	0.19486	1.99524	1.99524	1.99524	1.99524
	Zenkour 2013	$\neq 0$	0.19487	0.19487	0.19487	0.19487	2.00773	2.00773	2.00773	2.00773
	Akavci 2016	$= 0$	0.19605	0.19605	0.19605	0.19605	1.99516	1.99516	1.99516	1.99516
	Akavci 2016	$\neq 0$	0.19466	0.19466	0.19466	0.19466	2.07300	2.07300	2.07300	2.07300
	Present	$\neq 0$	0.19428	0.19428	0.19428	0.19428	2.12328	2.12328	2.12328	2.12328
1	Thai et al. 2014 (FSDT)	$= 0$	0.3064	0.2920	0.2809	0.2710	1.4517	1.3830	1.2775	1.2810
	Zenkour 2005a (FSDT)	$= 0$	0.30750	0.29301	0.28168	0.27167	1.45167	1.38303	1.27749	1.28096
	Zenkour 2005a (SSDT)	$= 0$	0.30624	0.29194	0.28082	0.27093	1.49859	1.42892	1.32342	1.32590
	Neves et al. 2012b	$= 0$	0.30900	0.29490	0.28380	0.27400	1.47420	1.40670	1.30260	1.30640
	Neves et al. 2012b	$\neq 0$	0.30700	0.29290	0.28200	0.27220	1.48130	1.41370	1.30920	1.31330
	Bessaim et al. 2013	$\neq 0$	0.30430	0.29007	0.27874	0.26915	1.46131	1.39243	1.28274	1.29030
	Zenkour 2013	$\neq 0$	0.30275	0.28867	0.27760	0.26815	1.48833	1.41781	1.30907	1.31204
	Akavci 2016	$= 0$	0.30627	0.29196	0.28083	0.27093	1.46322	1.39432	1.28879	1.29201
	Akavci 2016	$\neq 0$	0.30398	0.28977	0.27847	0.26891	1.52514	1.45397	1.34177	1.34783
	Present	$\neq 0$	0.30341	0.28923	0.27796	0.26842	1.56560	1.49282	1.37900	1.38399
2	Thai et al. 2014 (FSDT)	$= 0$	0.3526	0.3330	0.3163	0.3027	1.6750	1.5824	1.4253	1.4358
	Zenkour 2005a (FSDT)	$= 0$	0.35408	0.33441	0.31738	0.30370	1.67496	1.58242	1.42528	1.43580
	Zenkour 2005a (SSDT)	$= 0$	0.35218	0.33280	0.31611	0.30260	1.72412	1.63025	1.47387	1.48283
	Neves et al. 2012b	$= 0$	0.35420	0.33510	0.31860	0.30530	1.69200	1.60170	1.44760	1.45880
	Neves et al. 2012b	$\neq 0$	0.35190	0.33290	0.31640	0.30320	1.69940	1.60880	1.45430	1.46590
	Bessaim et al. 2013	$\neq 0$	0.35001	0.33068	0.31356	0.30060	1.68472	1.59170	1.42887	1.44497
	Zenkour 2013	$\neq 0$	0.34737	0.32816	0.31152	0.29874	1.72030	1.62591	1.46372	1.47421
	Akavci 2016	$= 0$	0.35222	0.33282	0.31613	0.30261	1.68708	1.59420	1.43723	1.44736
	Akavci 2016	$\neq 0$	0.34957	0.33030	0.31319	0.30031	1.75757	1.66237	1.49644	1.51084
	Present	$\neq 0$	0.34890	0.32966	0.31258	0.29974	1.80403	1.70704	1.53896	1.55206
10	Thai et al. 2014 (FSDT)	$= 0$	0.3894	0.3724	0.3492	0.3361	1.9216	1.8375	1.6160	1.6587
	Zenkour 2005a (FSDT)	$= 0$	0.40657	0.38787	0.36395	0.34996	1.92165	1.83754	1.61645	1.65844
	Zenkour 2005a (SSDT)	$= 0$	0.40376	0.38490	0.34916	0.34119	1.97313	1.88147	1.61979	1.64851
	Neves et al. 2012b	$= 0$	0.40510	0.38680	0.36370	0.35030	1.93160	1.84850	1.63270	1.67610
	Neves et al. 2012b	$\neq 0$	0.40260	0.38430	0.36120	0.34800	1.93970	1.85590	1.63950	1.68320
	Bessaim et al. 2013	$\neq 0$	0.40153	0.38303	0.35885	0.34591	1.93266	1.84705	1.61792	1.66754
	Zenkour 2013	$\neq 0$	0.39856	0.37924	0.35577	0.34259	1.97075	1.89162	2.18558	1.67350
	Akavci 2016	$= 0$	0.40390	0.38538	0.36204	0.34817	1.93451	1.84956	1.62871	1.67048
	Akavci 2016	$\neq 0$	0.40094	0.38248	0.35823	0.34549	2.01036	1.92481	1.69436	1.74262
	Present	$\neq 0$	0.40020	0.38171	0.35744	0.34477	2.06107	1.97490	1.74276	1.78991

3. Numerical results and discussions

3.1. Verification study

Because there are no works on studying the static bending and free vibration behavior of the bi-FGSW plates, the accuracy and efficiency of the present algorithm is verified by comparing the present results with the published results in some special cases. In this subsection, a sandwich plate made of one homogeneous ceramic core and two similar FGM face sheets is considered.

3.1.1. Static bending analysis
Firstly, an $Al/(ZrO_2)_1$ FGSW square plate subjected to double sinusoidally distributed load without elastic foundations is considered. The boundary conditions of the plate are simply supported at four edges. The dimensions of the plates are $a = b = 1$, $h = a/10$, $q = 1$. In Table 3, the dimensionless center deflection and dimensionless axial normal stress of FGSW square plate using

Table 4. The comparison of dimensionless center deflection of square FGSW plate resting on elastic foundations.

Scheme	k	Theory	ε_z	K_w, K_s			
				0,0	100,0	0,100	100,100
1-0-1	0	Taibi et al. 2015	$=0$	0.6813080	0.4052250	0.0836524	0.0771940
		Akavci 2016	$=0$	0.6813120	0.4052270	0.0724388	0.0675450
		Akavci 2016	$\neq 0$	0.6771950	0.4049670	0.0728693	0.0679580
		Present	$\neq 0$	0.6751195	0.4042514	0.0728568	0.0679438
	0.5	Taibi et al. 2015	$=0$	0.8867390	0.4699850	0.0861015	0.0792750
		Akavci 2016	$=0$	0.8866520	0.4699600	0.0742675	0.0691331
		Akavci 2016	$\neq 0$	0.8811670	0.4700280	0.0747292	0.0695684
		Present	$\neq 0$	0.8785358	0.4693057	0.0747197	0.0695609
	2	Taibi et al. 2015	$=0$	1.1099380	0.5260520	0.0878160	0.0807270
		Akavci 2016	$=0$	1.1095900	0.5259750	0.0755388	0.0702334
		Akavci 2016	$\neq 0$	1.1026700	0.5264450	0.0760263	0.0706912
		Present	$\neq 0$	1.0992631	0.5257032	0.0760205	0.0706871
3-1-3	0.5	Taibi et al. 2015	$=0$	0.8685960	0.4648390	0.0859270	0.0791280
		Akavci 2016	$=0$	0.8685190	0.4648170	0.0741378	0.0690208
		Akavci 2016	$\neq 0$	0.8631400	0.4648490	0.0745969	0.0694537
		Present	$\neq 0$	0.8605656	0.4641274	0.0745869	0.0694457
	2	Taibi et al. 2015	$=0$	1.0899700	0.5194610	0.0876306	0.0805702
		Akavci 2016	$=0$	1.0806600	0.5193880	0.0754013	0.0701146
		Akavci 2016	$\neq 0$	1.0738600	0.5197850	0.0758855	0.0705695
		Present	$\neq 0$	1.0705101	0.5190316	0.0758783	0.0705641
2-1-2	0.5	Taibi et al. 2015	$=0$	0.8604107	0.4624840	0.0858464	0.0790590
		Akavci 2016	$=0$	0.8603440	0.4624650	0.0740777	0.0689687
		Akavci 2016	$\neq 0$	0.8550140	0.4624810	0.0745356	0.0694005
		Present	$\neq 0$	0.8524641	0.4617600	0.0745253	0.0693923
	2	Taibi et al. 2015	$=0$	1.0663840	0.5160620	0.0875334	0.0804880
		Akavci 2016	$=0$	1.0660700	0.0515990	0.0753294	0.0700524
		Akavci 2016	$\neq 0$	1.0593400	0.5163580	0.0758117	0.7050560[a]
		Present	$\neq 0$	1.0560196	0.5155985	0.0758038	0.0704996
1-1-1	0.5	Taibi et al. 2015	$=0$	0.8389770	0.4562190	0.0856283	0.0788745
		Akavci 2016	$=0$	0.8389430	0.4562090	0.0739154	0.0688280
		Akavci 2016	$\neq 0$	0.8337460	0.4561850	0.0743699	0.0692568
		Present	$\neq 0$	0.8312618	0.4554658	0.0743591	0.0692481
	2	Taibi et al. 2015	$=0$	1.0243870	0.5060230	0.0872398	0.0872398
		Akavci 2016	$=0$	1.0241700	0.5059710	0.0751123	0.0698646
		Akavci 2016	$\neq 0$	1.0176600	0.5062460	0.0755889	0.0703128
		Present	$\neq 0$	1.0144538	0.5054779	0.0755793	0.0703051

[a] It should be 0.07050560.

the present algorithm are compared with other published solutions. The dimensionless center displacement is calculated by $\bar{w} = (10hE_0/qa^2)w(a/2, b/2, 0), E_0 = 1\text{GPa}$ and the dimensionless axial normal stress is calculated by $\bar{\sigma}_x = (10h^2/qa^2)\sigma_x(a/2, b/2, h/2)$. It is obvious that the present results are in good agreement with other higher-order and quasi-3D results for all cases of power-law index and scheme of the sandwich plates.

Next, the dimensionless center deflection of $\text{Ti} - 6\text{Al} - 4\text{V}/(\text{ZrO}_2)_3$ FGSW plate resting on elastic foundations subjected to sinusoidal distribution load using present hybrid quasi-3D theory and other theory are compared in Table 4. The dimensions of the plate and the loads are $a = b = 1$, $h = a/10$, $q = 100$. The dimensionless center displacement is calculated by $\bar{w} = (10^2 D_c/qa^4)w(a/2, b/2, 0)$, $K_w = k_w a^4/D_c$, $K_s = k_s a^2/D_c$ with $D_c = E_{ceramic}h^3/(12(1-\nu^2))$. The comparison shows that the present results are very closed to other published solutions of Taibi et al. (2015) and Akavci (2016).

3.1.2. Free vibration analysis
Table 5 presents the comparison of the dimensionless of the simply supported square $\text{Al}/\text{Al}_2\text{O}_3$ FGSW plate without elastic foundations using present hybrid quasi-3D theory and other

Table 5. The comparison of the dimensionless first ten frequencies of square FGSW plate.

Scheme	Theory	ε_z	Mode (α, β)									
			(1,1)	(1,2)	(2,2)	(1,3)	(2,3)	(1,4)	(3,3)	(2,4)	(3,4)	(4,4)
1-2-1	Thai et al. 2014 (FSDT)	$= 0$	1.3023	3.1563	4.9079	6.0262	7.6384	9.6811	10.1746	11.1430	13.4640	16.5076
	Zenkour 2005b (FSDT)	$= 0$	1.30020	3.14452	4.88021	5.98487	7.57215	9.57284	10.05424	10.99612	13.23801	16.13722
	Zenkour 2005b (SSDT)	$= 0$	1.30244	3.15686	4.90849	6.02622	7.63601	9.67121	10.16193	11.12321	13.41755	16.39820
	Meiche et al. 2011	$= 0$	1.30250	3.15726	4.90978	6.02866	7.64154	9.68465	10.17821	11.14644	13.46652	16.50693
	Akavci 2016	$= 0$	1.30244	3.15694	4.90901	6.02749	7.63966	9.68163	10.17490	11.14250	13.46070	16.49840
	Akavci 2016	$\neq 0$	1.30511	3.17001	4.93846	6.07048	7.70614	9.78411	10.28700	11.27470	13.64650	16.76500
	Present	$\neq 0$	1.30630	3.17290	4.94296	6.07603	7.71320	9.79312	10.29653	11.28510	13.65919	16.78069
2-2-1	Thai et al. 2014 (FSDT)	$= 0$	1.2436	3.0163	4.6932	5.7648	7.3110	9.2719	9.7459	10.6764	12.9084	15.8383
	Zenkour 2005b (FSDT)	$= 0$	1.26524	3.05968	4.74815	5.82264	7.36640	9.31198	9.78007	10.69588	12.87543	15.69346
	Zenkour 2005b (SSDT)	$= 0$	1.26780	3.07382	4.78065	5.87022	7.44002	9.42552	9.90439	10.84261	13.08260	15.99393
	Meiche et al. 2011	$= 0$	1.24375	3.01698	4.69456	5.76658	7.31319	9.27437	9.74847	10.67885	12.91005	15.83764
	Akavci 2016	$\neq 0$	1.24392	3.01795	4.69676	5.76977	7.31805	9.28169	9.75642	10.68810	12.92270	15.85500
	Akavci 2016	$\neq 0$	1.25087	3.04055	4.73990	5.82874	7.40333	9.40583	9.89083	10.84360	13.13360	16.14810
	Present	$\neq 0$	1.25212	3.04349	4.74436	5.83414	7.41005	9.41416	9.89955	10.85307	13.14476	16.16150

Table 6. The comparison of dimensionless of fundamental frequency of FGSW plate resting on elastic foundations.

a/h	k	K_w	K_s	Theory	2-1-2	1-1-1	2-2-1	1-2-1	1-0-1
5	0	0	0	Akavci 2016	1.19115	1.19115	1.19115	1.19115	1.19115
				Present	1.19245	1.19245	1.19245	1.19245	1.19245
		10	10	Akavci 2016	1.51351	1.51351	1.51351	1.51351	1.51351
				Present	1.51455	1.51455	1.51455	1.51455	1.51455
		100	100	Akavci 2016	3.09080	3.09084	3.09084	3.09084	3.09084
				Present	3.09084	3.09084	3.09084	3.09084	3.09084
	2	0	0	Akavci 2016	0.93179	0.95413	0.97549	0.99274	0.90884
				Present	0.93266	0.95509	0.97651	0.99380	0.90966
		10	10	Akavci 2016	1.33409	1.34691	1.36107	1.37133	1.32314
				Present	1.33493	1.34784	1.36204	1.37236	1.32389
		100	100	Akavci 2016	2.68234	2.75786	2.79373	2.84764	2.56208
				Present	2.68234	2.75786	2.79437	2.84764	2.56208
	10	0	0	Akavci 2016	0.87914	0.89688	0.92151	0.93562	0.86327
				Present	0.87982	0.89771	0.92251	0.93663	0.86396
		10	10	Akavci 2016	1.30448	1.31193	1.32742	1.33389	1.30224
				Present	1.30508	1.31271	1.32837	1.33489	1.30276
		100	100	Akavci 2016	2.50435	2.61784	2.67072	2.74945	2.31764
				Present	2.50435	2.61784	2.67176	2.74945	2.31764
10	0	0	0	Akavci 2016	1.29692	1.29692	1.29692	1.29692	1.29692
				Present	1.29834	1.29834	1.29834	1.29834	1.29834
		10	10	Akavci 2016	1.61603	1.61603	1.61603	1.61603	1.61603
				Present	1.61718	1.61718	1.61718	1.61718	1.61718
		100	100	Akavci 2016	3.31161	3.31161	3.31161	3.31161	3.31161
				Present	3.31215	3.31215	3.31215	3.31215	3.31215
	2	0	0	Akavci 2016	0.99389	1.01785	1.04293	1.06150	0.97214
				Present	0.99498	1.01898	1.04409	1.06265	0.97319
		10	10	Akavci 2016	1.40287	1.41684	1.43347	1.44479	1.39245
				Present	1.40369	1.41770	1.43437	1.44570	1.39321
		100	100	Akavci 2016	3.28172	3.27584	3.27742	3.37358	3.29568
				Present	3.28227	3.27647	3.27807	3.27427	3.29615
	10	0	0	Akavci 2016	0.93742	0.95372	0.98239	0.99572	0.93086
				Present	0.93841	0.95481	0.98362	0.99689	0.93181
		10	10	Akavci 2016	1.37067	1.37733	1.39522	1.40137	1.37339
				Present	1.37137	1.37813	1.39614	1.40227	1.37404
		100	100	Akavci 2016	3.29462	3.28050	3.28023	3.27038	3.32236
				Present	3.29496	3.28099	3.28085	3.27107	3.32260
100	0	0	0	Akavci 2016	1.34038	1.34038	1.34038	1.34038	1.34038
				Present	1.34184	1.34184	1.34184	1.34184	1.34184
		10	10	Akavci 2016	1.65899	1.65899	1.65899	1.65899	1.65899
				Present	1.66017	1.66017	1.66017	1.66017	1.66017
		100	100	Akavci 2016	3.36942	3.36942	3.36942	3.36942	3.36942
				Present	3.37000	3.37000	3.37000	3.37000	3.37000
	2	0	0	Akavci 2016	1.01820	1.04279	1.06946	1.08854	0.99710
				Present	1.01939	1.04399	1.07068	1.08973	0.99825
		10	10	Akavci 2016	1.43000	1.44444	1.46227	1.47402	1.42000
				Present	1.43084	1.44531	1.46316	1.47490	1.42081
		100	100	Akavci 2016	3.33441	3.32829	3.32997	3.32610	3.34906
				Present	3.33477	3.32866	3.33036	3.32649	3.34940
	10	0	0	Akavci 2016	0.96024	0.97582	1.00620	1.01911	0.95802
				Present	0.96136	0.97703	1.00752	1.02036	0.95908
		10	10	Akavci 2016	1.39670	1.40285	1.42192	1.42781	1.40234
				Present	1.39747	1.40369	1.42286	1.42869	1.40307
		100	100	Akavci 2016	3.34801	3.33315	3.33266	3.32250	3.37718
				Present	3.34833	3.33350	3.33306	3.32288	3.37748

published results of Thai et al. (2014), Zenkour (2005b), Meiche et al. (2011) and Akavci (2016). The dimensionless of the frequency is calculated by $\bar{\omega} = \omega a^2 / \left(h\sqrt{\rho_0/E_0} \right)$. It can be seen from Table 5 that the present results are in excellent agreement with other published results.

Table 7. The dimensionless center deflection $w^*(z = 0)$ of the bi-FGSW platesof type A resting on elastic foundations.

a/b	a/h	k	Scheme							
			1-0-1	1-1-1	1-2-1	2-1-2	2-1-1	1-1-2	2-2-1	1-2-2
1	10	0	0.19994	0.19994	0.19994	0.19994	0.19994	0.19994	0.19994	0.19994
		1	0.08425	0.09504	0.10427	0.08977	0.09404	0.09380	0.10087	0.10051
		2	0.07492	0.08401	0.09272	0.07935	0.08328	0.08326	0.08954	0.08941
		10	0.06897	0.07456	0.08184	0.07131	0.07452	0.07470	0.07938	0.07952
	20	0	0.33170	0.33170	0.33170	0.33170	0.33170	0.33170	0.33170	0.33170
		1	0.25377	0.26432	0.27317	0.25918	0.26410	0.26418	0.27053	0.27042
		2	0.24227	0.25177	0.26096	0.24685	0.25203	0.25245	0.25851	0.25874
		10	0.23500	0.24036	0.24836	0.23700	0.24161	0.24235	0.24689	0.24757
2	10	0	0.33905	0.33905	0.33905	0.33905	0.33905	0.33905	0.33905	0.33905
		1	0.17441	0.19148	0.20622	0.18312	0.19046	0.19031	0.20126	0.20086
		2	0.15836	0.17285	0.18700	0.16537	0.17237	0.17263	0.18244	0.18250
		10	0.14836	0.15685	0.16862	0.15176	0.15758	0.15821	0.16542	0.16599
	20	0	0.19994	0.19994	0.19994	0.19994	0.19994	0.19994	0.19994	0.19994
		1	0.08425	0.09504	0.10427	0.08977	0.09404	0.09380	0.10087	0.10051
		2	0.07492	0.08401	0.09272	0.07935	0.08328	0.08326	0.08954	0.08941
		10	0.06897	0.07456	0.08184	0.07131	0.07452	0.07470	0.07938	0.07952

Table 8. The dimensionless axial normal stress $\sigma_x^*(z = h/2)$ of the bi-FGSW platesof type A resting on elastic foundations.

a/b	a/h	k	Scheme							
			1-0-1	1-1-1	1-2-1	2-1-2	2-1-1	1-1-2	2-2-1	1-2-2
1	10	0	1.03251	1.03251	1.03251	1.03251	1.03251	1.03251	1.03251	1.03251
		1	2.10827	2.29945	2.49523	2.20086	2.54361	2.11336	2.72058	2.21054
		2	1.90643	2.04620	2.21264	1.96925	2.26876	1.90515	2.43193	1.97427
		10	1.80473	1.86009	1.97760	1.81929	2.03867	1.78761	2.17703	1.81257
	20	0	0.88104	0.88104	0.88104	0.88104	0.88104	0.88104	0.88104	0.88104
		1	3.34147	3.42615	3.52001	3.38054	3.80322	3.14020	3.91119	3.15959
		2	3.22326	3.28238	3.36838	3.24622	3.64386	3.03530	3.76621	3.03090
		10	3.17393	3.17598	3.23433	3.16344	3.46681	3.01609	3.60087	2.96742
2	10	0	1.41105	1.41105	1.41105	1.41105	1.41105	1.41105	1.41105	1.41105
		1	3.65921	3.92497	4.19713	3.78743	4.32815	3.61644	4.57651	3.74381
		2	3.36121	3.55770	3.79599	3.44831	3.93293	3.31739	4.17153	3.40533
		10	3.21220	3.28228	3.45151	3.22640	3.58770	3.15504	3.79813	3.17481
	20	0	1.03251	1.03251	1.03251	1.03251	1.03251	1.03251	1.03251	1.03251
		1	2.10827	2.29945	2.49523	2.20086	2.54361	2.11336	2.72058	2.21054
		2	1.90643	2.04620	2.21264	1.96925	2.26876	1.90515	2.43193	1.97427
		10	1.80473	1.86009	1.97760	1.81929	2.03867	1.78761	2.17703	1.81257

Table 9. The dimensionless transverse shear stress $\tau_{xz}^*(z = 0)$ of the bi-FGSW platesof type A resting on elastic foundations.

a/b	a/h	k	Scheme							
			1-0-1	1-1-1	1-2-1	2-1-2	2-1-1	1-1-2	2-2-1	1-2-2
1	10	0	0.11030	0.11030	0.11030	0.11030	0.11030	0.11030	0.11030	0.11030
		1	0.07627	0.11260	0.13128	0.09676	0.09820	0.09241	0.11547	0.11049
		2	0.06034	0.09867	0.12345	0.08077	0.08298	0.07687	0.10305	0.09707
		10	0.04138	0.07549	0.10477	0.05827	0.06134	0.05588	0.08124	0.07493
	20	0	0.04753	0.04753	0.04753	0.04753	0.04753	0.04753	0.04753	0.04753
		1	0.06141	0.08554	0.09441	0.07569	0.07447	0.06996	0.08426	0.08060
		2	0.05177	0.08078	0.09601	0.06780	0.06759	0.06238	0.08104	0.07612
		10	0.03680	0.06568	0.08762	0.05146	0.05283	0.04786	0.06818	0.06255
2	10	0	0.11914	0.11914	0.11914	0.11914	0.11914	0.11914	0.11914	0.11914
		1	0.10198	0.14807	0.16986	0.12832	0.12909	0.12143	0.15008	0.14361
		2	0.08209	0.13250	0.16339	0.10921	0.11129	0.10301	0.13685	0.12881
		10	0.05683	0.10304	0.14148	0.07987	0.08353	0.07598	0.10984	0.10118
	20	0	0.11030	0.11030	0.11030	0.11030	0.11030	0.11030	0.11030	0.11030
		1	0.07627	0.11260	0.13128	0.09676	0.09820	0.09241	0.11547	0.11049
		2	0.06034	0.09867	0.12345	0.08077	0.08298	0.07687	0.10305	0.09707
		10	0.04138	0.07549	0.10477	0.05827	0.06134	0.05588	0.08124	0.07493

Table 10. The dimensionless center deflection $w^*(z = 0)$ of the bi-FGSW platesof type B resting on elastic foundations.

a/b	a/h	k	Scheme							
			1-0-1	1-1-1	1-2-1	2-1-2	2-1-1	1-1-2	2-2-1	1-2-2
1	10	0	0.06364	0.06364	0.06364	0.06364	0.06364	0.06364	0.06364	0.06364
		1	0.10518	0.09440	0.08749	0.09922	0.09236	0.10000	0.08764	0.09408
		2	0.12328	0.10827	0.09796	0.11521	0.10402	0.11708	0.09742	0.10836
		10	0.14319	0.12752	0.11363	0.13548	0.11880	0.13865	0.11064	0.12878
	20	0	0.22422	0.22422	0.22422	0.22422	0.22422	0.22422	0.22422	0.22422
		1	0.27444	0.26434	0.25692	0.26906	0.26216	0.26975	0.25706	0.26398
		2	0.28872	0.27728	0.26792	0.28288	0.27349	0.28424	0.26735	0.27732
		10	0.30105	0.29184	0.28173	0.29686	0.28552	0.29866	0.27923	0.29262
2	10	0	0.13826	0.13826	0.13826	0.13826	0.13826	0.13826	0.13826	0.13826
		1	0.21068	0.19320	0.18149	0.20112	0.18971	0.20235	0.18172	0.19263
		2	0.23852	0.21573	0.19912	0.22649	0.20889	0.22928	0.19819	0.21584
		10	0.26663	0.24497	0.22415	0.25632	0.23186	0.26066	0.21942	0.24676
	20	0	0.06364	0.06364	0.06364	0.06364	0.06364	0.06364	0.06364	0.06364
		1	0.10518	0.09440	0.08749	0.09922	0.09236	0.10000	0.08764	0.09408
		2	0.12328	0.10827	0.09796	0.11521	0.10402	0.11708	0.09742	0.10836
		10	0.14319	0.12752	0.11363	0.13548	0.11880	0.13865	0.11064	0.12878

Table 11. The dimensionless normal stress $\sigma_x^*(z = h/2)$ of the bi-FGSW platesof type B resting on elastic foundations.

a/b	a/h	k	Scheme							
			1-0-1	1-1-1	1-2-1	2-1-2	2-1-1	1-1-2	2-2-1	1-2-2
1	10	0	1.75027	1.75027	1.75027	1.75027	1.75027	1.75027	1.75027	1.75027
		1	0.63298	0.55423	0.50642	0.58850	0.51625	0.62403	0.48687	0.57669
		2	0.77754	0.65553	0.58085	0.70894	0.59017	0.77310	0.54675	0.69668
		10	0.97769	0.80810	0.69761	0.88252	0.69577	0.98733	0.63279	0.88594
	20	0	3.16981	3.16981	3.16981	3.16981	3.16981	3.16981	3.16981	3.16981
		1	0.83973	0.78896	0.75694	0.81108	0.74540	0.85628	0.72680	0.82324
		2	0.92451	0.85133	0.80662	0.88252	0.78767	0.95271	0.76198	0.90488
		10	1.04771	0.93580	0.87576	0.97961	0.84798	1.07944	0.80939	1.01966
2	10	0	3.13419	3.13419	3.13419	3.13419	3.13419	3.13419	3.13419	3.13419
		1	1.00140	0.89650	0.83106	0.94254	0.84033	0.99508	0.80015	0.93137
		2	1.18434	1.02950	0.93172	1.09778	0.93767	1.18740	0.88028	1.09002
		10	1.42884	1.21946	1.08246	1.31051	1.07249	1.44813	0.99149	1.32602
	20	0	1.75027	1.75027	1.75027	1.75027	1.75027	1.75027	1.75027	1.75027
		1	0.63298	0.55423	0.50642	0.58850	0.51625	0.62403	0.48687	0.57669
		2	0.77754	0.65553	0.58085	0.70894	0.59017	0.77310	0.54675	0.69668
		10	0.97769	0.80810	0.69761	0.88252	0.69577	0.98733	0.63279	0.88594

Table 12. The dimensionless transverse shear stress $\tau_{xz}^*(z = 0)$ of the bi-FGSW platesof type B resting on elastic foundations.

a/b	a/h	k	Scheme							
			1-0-1	1-1-1	1-2-1	2-1-2	2-1-1	1-1-2	2-2-1	1-2-2
1	10	0	0.19705	0.19705	0.19705	0.19705	0.19705	0.19705	0.19705	0.19705
		1	0.21855	0.19809	0.19491	0.20371	0.20317	0.20834	0.19817	0.19989
		2	0.23390	0.19778	0.19316	0.20692	0.20714	0.21370	0.19887	0.20010
		10	0.31046	0.20245	0.19119	0.22622	0.22334	0.24012	0.20416	0.20547
	20	0	0.18012	0.18012	0.18012	0.18012	0.18012	0.18012	0.18012	0.18012
		1	0.14596	0.14203	0.14683	0.14136	0.14788	0.14388	0.14918	0.14368
		2	0.13985	0.12922	0.13507	0.12954	0.13925	0.13238	0.13966	0.13070
		10	0.16724	0.11780	0.12070	0.12615	0.13702	0.13181	0.13147	0.11876
2	10	0	0.27252	0.27252	0.27252	0.27252	0.27252	0.27252	0.27252	0.27252
		1	0.27681	0.25640	0.25595	0.26109	0.26415	0.26663	0.26018	0.25892
		2	0.28581	0.24879	0.24815	0.25674	0.26291	0.26422	0.25581	0.25169
		10	0.36576	0.24511	0.23787	0.26987	0.27527	0.28484	0.25563	0.24820
	20	0	0.19705	0.19705	0.19705	0.19705	0.19705	0.19705	0.19705	0.19705
		1	0.21855	0.19809	0.19491	0.20371	0.20317	0.20834	0.19817	0.19989
		2	0.23390	0.19778	0.19316	0.20692	0.20714	0.21370	0.19887	0.20010
		10	0.31046	0.20245	0.19119	0.22622	0.22334	0.24012	0.20416	0.20547

Table 13. The dimensionless center deflection $w^*(z = h/2)$ of square bi-FGSW platesof type A resting on elastic foundations.

Scheme	K_w, K_s								
	0,0	0,5	0,10	50,0	50,5	50,10	100,0	100,5	100,10
1-0-1	0.10900	0.09932	0.09121	0.10387	0.09504	0.08759	0.09920	0.09111	0.08425
1-1-1	0.12778	0.11467	0.10400	0.12078	0.10900	0.09932	0.11451	0.10387	0.09504
1-2-1	0.14503	0.12838	0.11515	0.13609	0.12132	0.10944	0.12818	0.11500	0.10427
2-1-2	0.11843	0.10708	0.09772	0.11240	0.10213	0.09358	0.10695	0.09761	0.08977
1-8-1	0.21635	0.18129	0.15601	0.19705	0.16754	0.14572	0.18091	0.15573	0.13670
8-1-8	0.11133	0.10125	0.09284	0.10598	0.09680	0.08909	0.10113	0.09274	0.08563
2-1-1	0.12597	0.11321	0.10280	0.11917	0.10769	0.09822	0.11306	0.10267	0.09404
1-1-2	0.12555	0.11287	0.10252	0.11879	0.10738	0.09796	0.11272	0.10239	0.09380
2-2-1	0.13855	0.12327	0.11103	0.13036	0.11675	0.10571	0.12309	0.11088	0.10087
1-2-2	0.13788	0.12274	0.11059	0.12977	0.11627	0.10531	0.12256	0.11045	0.10051

Table 14. The dimensionless center deflection $w^*(z = h/2)$ of the square bi-FGSW platesof type B resting on elastic foundations.

Scheme	K_w, K_s								
	0,0	0,5	0,10	50,0	50,5	50,10	100,0	100,5	100,10
1-0-1	0.56318	0.49587	0.44293	0.52695	0.46756	0.42020	0.49509	0.44231	0.39969
1-1-1	0.48516	0.43436	0.39319	0.45802	0.41248	0.37518	0.43376	0.39270	0.35874
1-2-1	0.43832	0.39643	0.36185	0.41605	0.37813	0.34654	0.39593	0.36143	0.33247
2-1-2	0.51920	0.46145	0.41526	0.48825	0.43684	0.39522	0.46077	0.41471	0.37702
1-8-1	0.34961	0.32243	0.29917	0.33529	0.31021	0.28863	0.32210	0.29889	0.27880
8-1-8	0.55113	0.48650	0.43544	0.51637	0.45922	0.41345	0.48574	0.43483	0.39358
2-1-1	0.47103	0.42300	0.38386	0.44541	0.40222	0.36667	0.42243	0.38339	0.35096
1-1-2	0.52488	0.46592	0.41887	0.49326	0.44083	0.39848	0.46523	0.41831	0.37999
2-2-1	0.43932	0.39725	0.36253	0.41695	0.37887	0.34716	0.39675	0.36212	0.33304
1-2-2	0.48294	0.43257	0.39172	0.45604	0.41086	0.37383	0.43198	0.39123	0.35751

Continuously, the comparison of the dimensionless fundamental frequency of simply supported square $Al/(ZrO_2)_1$ FGSW plate resting on the elastic foundations using hybrid quasi-3D theory and the published results of Akavci (2016). The dimensionless of the frequency is computed by $\bar{\omega} = \omega a^2/\left(h\sqrt{\rho_0/E_0}\right)$. It can be concluded that the differences between the present results and the results of Akavci are very small (Table 6).

3.2. Parameter study

In this section, the bending and free vibration of the fully simple supported bi-FGSW plates resting on elastic foundations are investigated. The structures and material properties of the two types of bi-FGSW plates are given in Tables 1 and 2. For the static bending problem, the plates are subjected to sinusoidal load of $q = q_0 \sin(\pi x/a) \sin(\pi y/b)$; for the free vibration problem, the plates are free of the force action. For convenience, the following dimensionless quantities are used

$$w^*(z) = \frac{10h_0 E_0}{a^2 q_0} w\left(\frac{a}{2}, \frac{b}{2}, z\right), \sigma_x^*(z) = \frac{10h_0^2}{a^2 q_0} \sigma_x\left(\frac{a}{2}, \frac{b}{2}, z\right),$$

$$\tau_{xz}^*(z) = \frac{h_0}{q_0 a} \tau_{xz}\left(0, \frac{b}{2}, z\right), \omega^* = \omega \frac{a^2}{h_0} \sqrt{\frac{\rho_0}{E_0}}, K_w = k_w \frac{a^4}{D_0}, K_s = k_s \frac{a^2}{D_0}, \tag{32}$$

$$D_0 = \frac{10^2 E_0 h_0^3}{12(1 - \nu^2)}, E_0 = 1\text{GPa}, \rho_0 = 1\text{kg/m}^3, h_0 = a/10, a = 1, q_0 = 1.$$

a) (1-2-1) Type A

b) (2-2-1) Type A

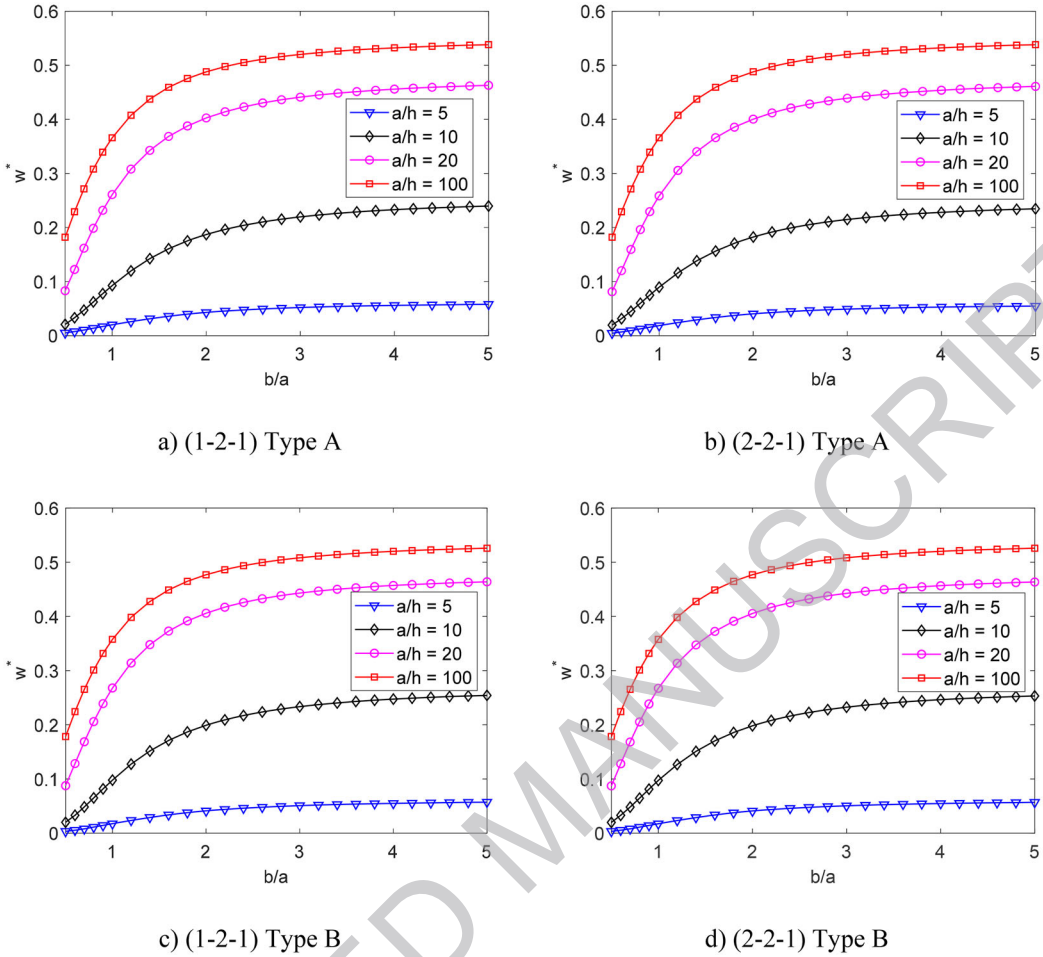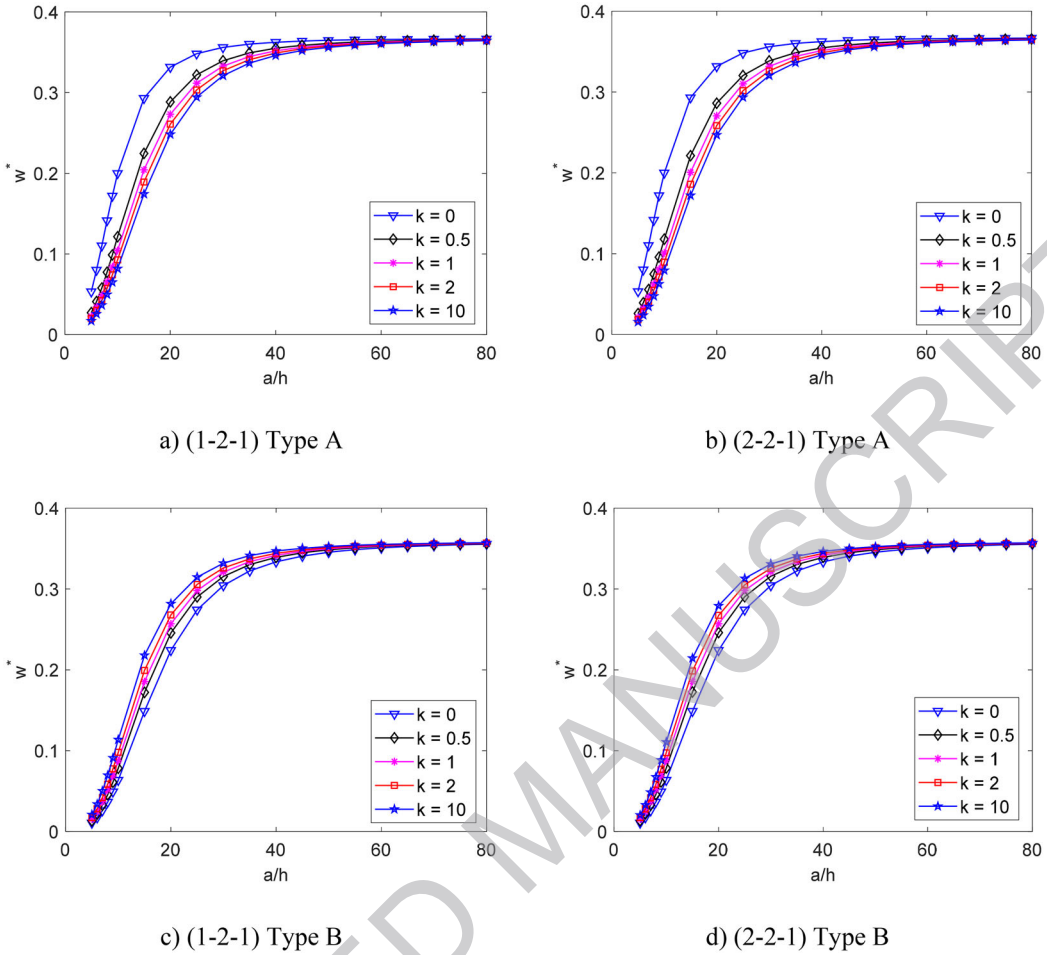c) (1-2-1) Type B

d) (2-2-1) Type B

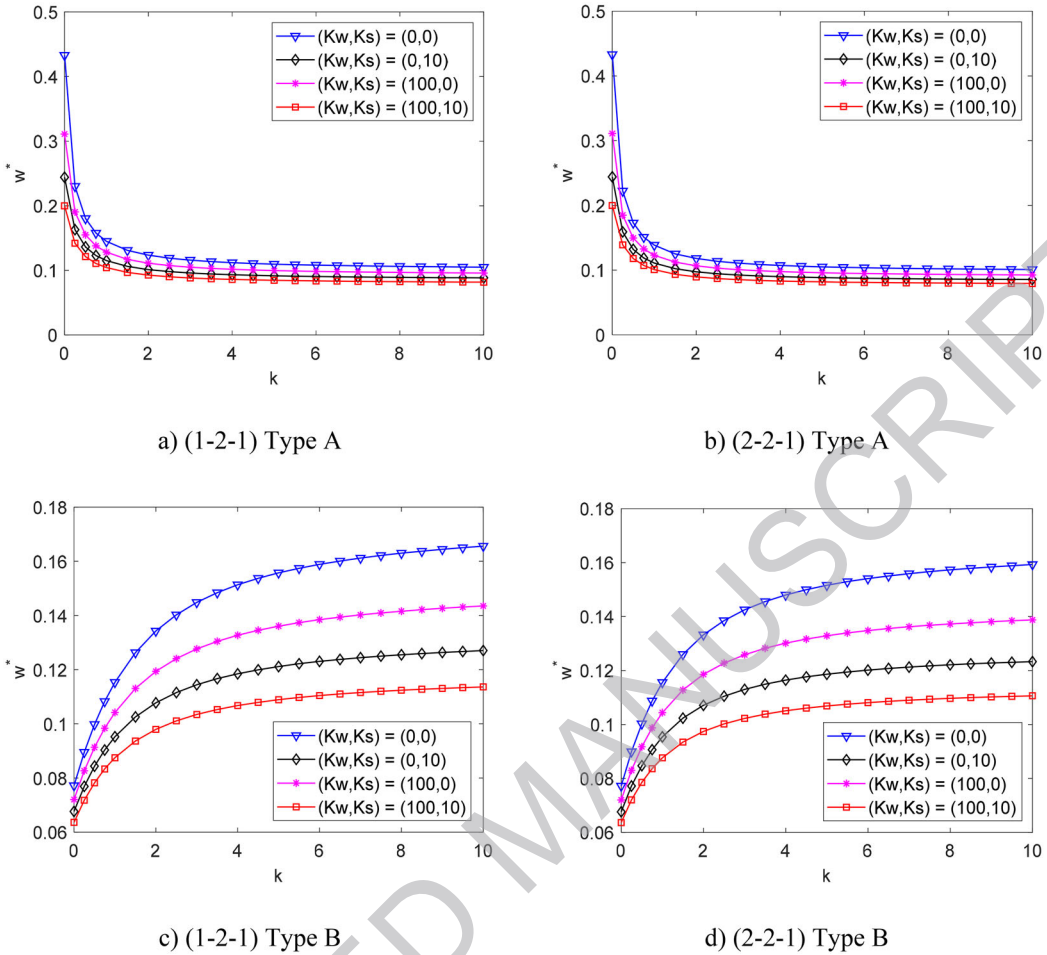**Figure 3.** The variation of the dimensionless center deflection w^* of the bi-FGSW plates as the function of aspect ratio.

3.2.1. Static bending analysis of bi-FGSW plate

Firstly, the effects of some parameters on the bending of the bi-FGSW plate subjected to the sinusoidal load are examined. The dimensionless center deflection, normal stress and transverse shear stress of the bi-FGSW plate of type A are given in Tables 7-9, while those of the bi-FGSW plate of type B are given in Tables 10-12. Two dimensionless parameters of the elastic foundations are $K_w = 100, K_s = 10$. It is obvious that when the power-law index increases, the deflections of the bi-FGSW plates of type A decreases while the deflection of the bi-FGSW plates of type B increases. The reason is that when the power-law index increases, the effective Young's modulus of the materials of two face sheets increases in the case of bi-FGSW plates of type A. Oppositely, the effective Young's modulus of the materials of two face sheets decreases due to the increasing of the power-law index in the case of bi-FGSW plates of type B as shown in Fig. 2.

The dimensionless center deflections of square bi-FGSW plates of type A and type B with different values of the elastic foundation's parameters are presented in Table 13 and 14. The dimensions of the plate are $a = b$, $a/h = 10$, $k = 2$. According to these tables, the elastic foundations affect significantly on the displacement of the bi-FGSW plates. When the stiffnesses of the elastic foundations increase, the center deflections of the bi-FGSW plates decreases because the stiffness of the system increases. With similar the power-law index, parameters of elastic foundations and scheme of skin-core-skin thicknesses ratio, the center deflections of the bi-FGSW plates of type A

Figure 4. The variation of the dimensionless center deflection w^* of the square bi-FGSW plates as the function of side-to-thickness ratio.

are much smaller than those of type B, because the bi-FGSW plates of type A consist of ceramic core while the bi-FGSW plates of type B consist of metal core.

Next, we investigate the influence of the aspect ratio b/a on the static bending of the bi-FGSW plates. The bi-FGSW plate of type A and B with the material parameter of $k = 2$ and the foundation parameters of $K_w = 100, K_s = 10$ are considered herein. The aspect ratio b/a changes from 0.5 to 3. The variation of the center deflection of the bi-FGSW plates as the function of the aspect ratio b/a is presented in Fig. 3. According to Fig. 3, it is obvious that the center deflections of the bi-FGSW plates of type A and B increases as increasing of the aspect ratio b/a. The dimensionless deflections of the bi-FGSW plates of type A and B with small values of the side-to-thickness ratio are greater than the deflection of the bi-FGSW plate with higher values of the side-to-thickness ratio. When the side-to-thickness ratio, the aspect ratio, the power-law index and the scheme of two types of the bi-FGSW plate are similar, the deflections of the bi-FGSW plates of type A are greater than those of type B. It is because the core layer of the bi-FGSW plates of type A is made of hard homogeneous ceramic while the core layer of the bi-FGSW plates is made of soft homogeneous metal.

Continuously, Fig. 4 demonstrates the dependence of the center deflection of the bi-FGSW plates on the change of the side-to-thickness ratio. The side-to-thickness ratio change in the range

Figure 5. The variation of the dimensionless center deflection w^* of the square bi-FGSW plates as the function of power-law index.

of $5 \leq a/h \leq 80$, the aspect ratio of $b/a = 1$, the elastic foundation parameters of $K_w = 100, K_s = 10$. It can see clearly that when the side-to-thickness ratio increases, the center deflections of the bi-FGSW plates increase. Because of when side-to-thickness ratio increases, the thickness of the plates decreases, so the stiffness of the plates decreases. When the side-to-thickness ratio varies from 5 to 20, the deflections increase rapidly and when the side-to-thickness ratio is greater than 20, the speed of the increase is slower. When the side-to-thickness ratio is greater than 60, the deflections of the bi-FGSW plate is almost unchanged. It is because when the side-to-thickness ratio is small, the stiffness of the plate is much greater than the stiffness of the elastic foundations, so the variation of the side-to-thickness affects strongly on the deflection of the plate. When this ratio is high, the stiffness of the plate is very small in comparison with the stiffness of the elastic foundations, so it can be negligible when calculating the stiffness of the system of plate-elastic foundations, so the deflection of the plate depends strongly on the stiffness of the elastic foundations which is unchanged.

Next, the variation of the dimensionless of the center deflection of the square bi-FGSW plates as the function of the power-law index k is demonstrated in Fig. 5. The side-to-thickness ratio of the plates is $a/h = 10$, while the power-law index k varies from 0 to 10. Figure 5 shows that the deflections of the bi-FGSW plates of type A decrease as the increase of the power-law index. On the contrary, the deflections of the bi-FGSW plate of type B increase when the power-law index
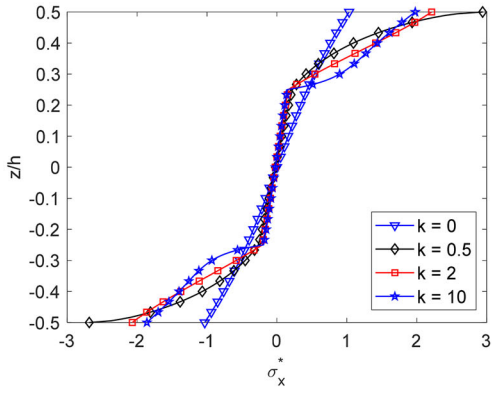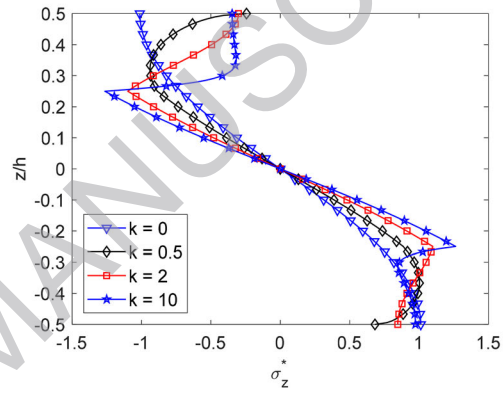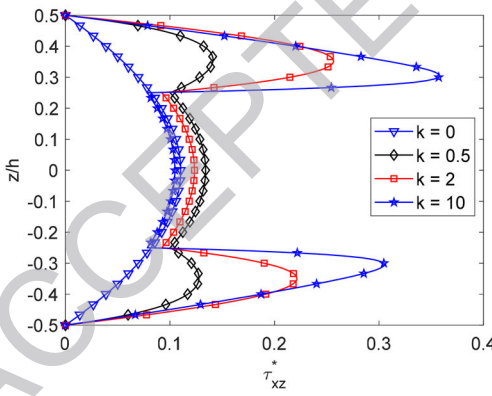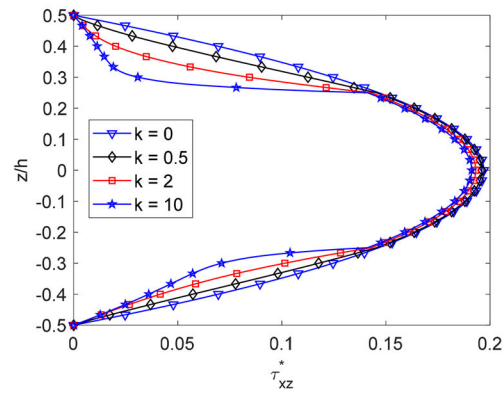
a) (1-2-1) Type A
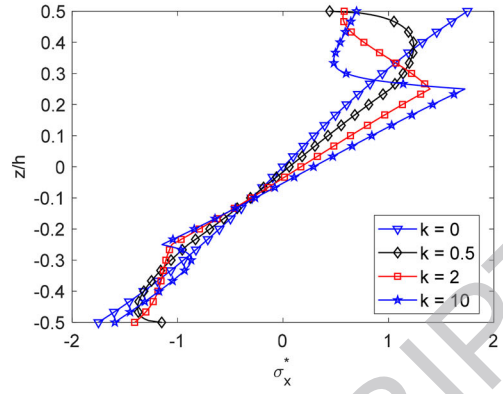
b) (1-2-1) Type B
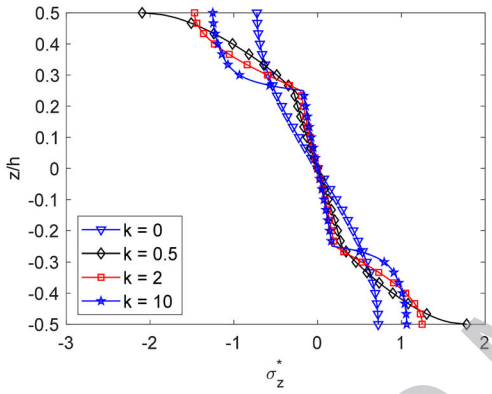
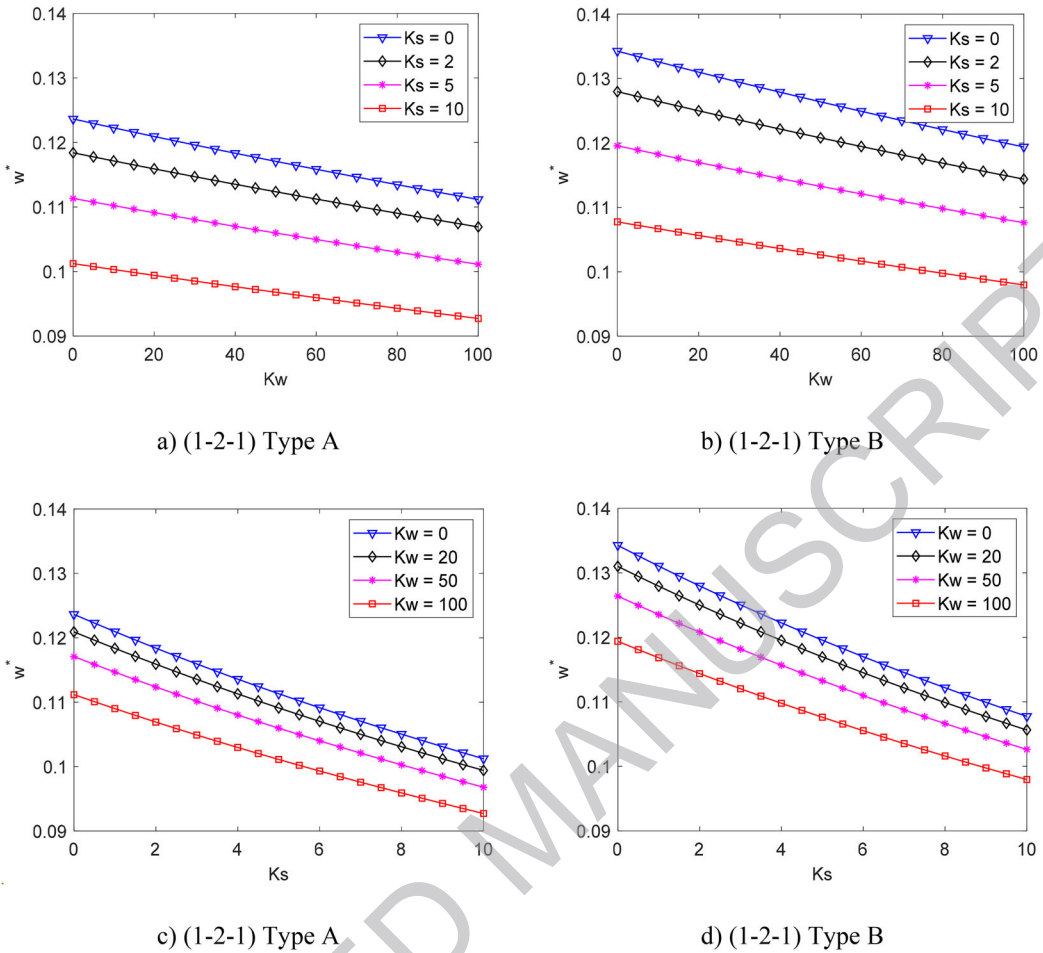c) (1-2-1) Type A

d) (1-2-1) Type B

e) (1-2-1) Type A

f) (1-2-1) Type B

Figure 6. The distribution of the normal and shear stresses through the thickness of the square bi-FGSW plates with different values of the power-law indexes.

Figure 7. The effects of the elastic foundation parameters on the dimensionless center deflection w^* of the square bi-FGSW plates.

increases. The reason is that when the power-law index of the bi-FGSW plate of type A increases, the stiffness of such plate increases as shown in Fig. 2. In the case of bi-FGSW plates of type B, when the power-law index increases, the effective Young's modulus of the plates decreases, so the center deflections of the plates increase.

Besides, the effects of the power-law index on the distribution of the normal and shear stresses of bi-FGSW plates are demonstrated in Fig. 6. For both type of A and B of the bi-FGSW plates, the distribution of the axial normal stresses, normal stresses and transverse shear stresses through the thickness of the bi-FGSW plates are asymmetric when the power-law index $k > 0$. When the power-law index $k = 0$, the distributions of the stresses through the thickness are symmetric. Because two face sheets of the bi-FGSW plate are made of two different types of FGM layer with different ingredients. So (1-2-1) bi-FGSW plate becomes symmetric sandwich plate when $k = 0$ and it becomes asymmetric one when $k > 0$. So, the bi-FGSW plates can be used in some special cases to avoid the stresses concentration at the surface of the plates.

The effects of the elastic foundation's parameters on the bending of the square bi-FGSW plates are demonstrated in Figs. 7 and 8. In Figure 7, the dependence of the dimensionless center deflection of the bi-FGSW plate on two parameters of the elastic foundations are presented. The deflection of the bi-FGSW plate can be reduced by the increase of the parameters of the elastic
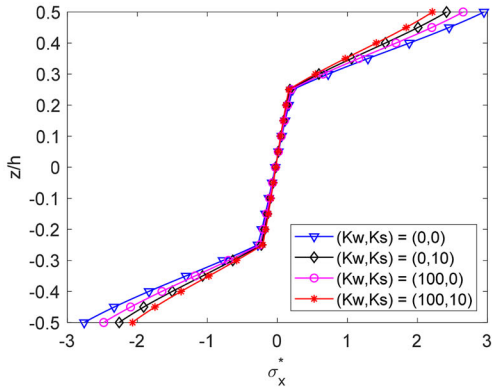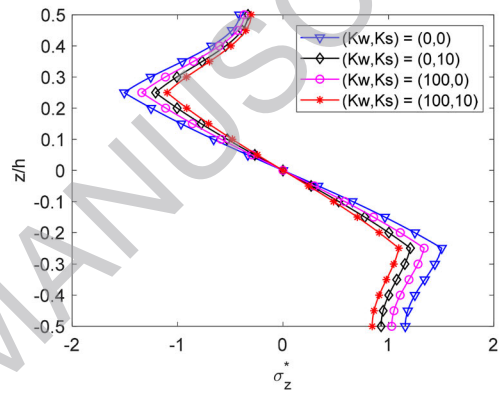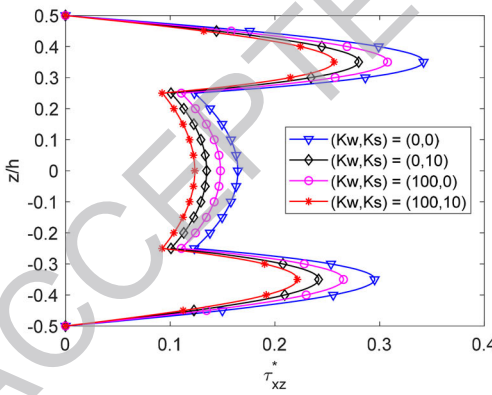
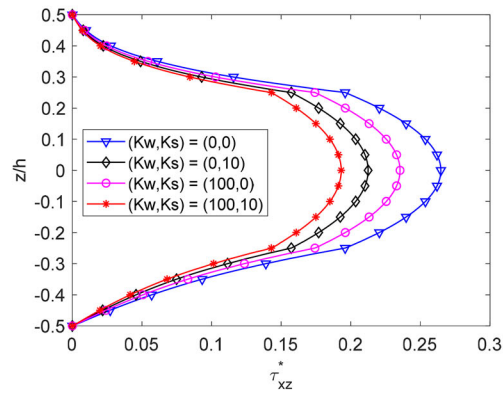a) (1-2-1) Type A
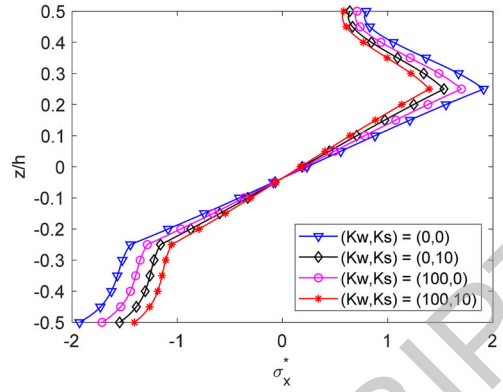
b) (1-2-1) Type B
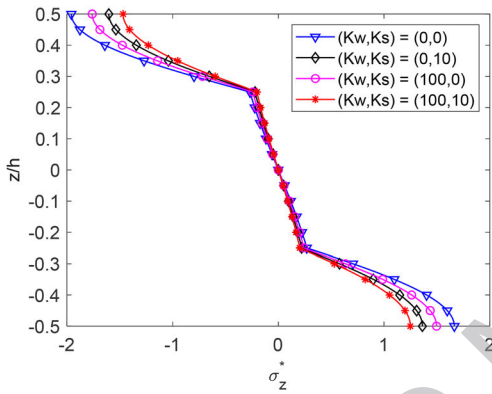
c) (1-2-1) Type A

d) (1-2-1) Type B

e) (1-2-1) Type A

f) (1-2-1) Type B

Figure 8. The distribution of the normal and shear stresses through the thickness of the square bi-FGSW plates with different values of elastic foundation parameters.

Table 15. The dimensionless first nine frequencies ω^* of the square bi-FGSW platesof type A resting on elastic foundations.

Scheme	a/h	k	Mode (α, β)								
			(1,1)	(1,2)	(2,2)	(1,3)	(2,3)	(1,4)	(3,3)	(2,4)	(3,4)
1-1-1	10	0	1.05407	2.01847	2.92697	3.50032	4.31741	5.33780	5.58207	6.05894	7.19028
		1	1.58808	3.34227	4.88931	5.82837	7.12759	8.69828	9.06715	9.78038	11.44072
		2	1.71099	3.64106	5.34036	6.37132	7.79722	9.52047	9.92509	10.70735	12.52804
		10	1.85112	4.00804	5.92870	7.10238	8.73444	10.71810	11.18536	12.09016	14.20223
	20	0	1.16506	1.79827	2.37253	2.73785	3.26760	3.94770	4.11379	4.44177	5.23953
		1	1.35403	2.38220	3.37172	4.00902	4.93346	6.11220	6.39803	6.95978	8.31060
		2	1.40529	2.52580	3.60893	4.30722	5.32053	6.61291	6.92631	7.54227	9.02345
		10	1.46618	2.68985	3.88232	4.65462	5.77962	7.22111	7.57172	8.26192	9.92737
1-2-1	10	0	1.05407	2.01847	2.92697	3.50032	4.31741	5.33780	5.58207	6.05894	7.19028
		1	1.50206	3.12189	4.54519	5.40695	6.59693	8.03265	8.36943	9.02024	10.53370
		2	1.60822	3.36816	4.90193	5.82660	7.09959	8.63069	8.98922	9.68149	11.28887
		10	1.73593	3.68124	5.37820	6.40227	7.81317	9.51144	9.90928	10.67761	12.46220
	20	0	1.16506	1.79827	2.37253	2.73785	3.26760	3.94770	4.11379	4.44177	5.23953
		1	1.31946	2.28393	3.20644	3.79902	4.65698	5.74870	6.01309	6.53236	7.77930
		2	1.36275	2.40773	3.40982	4.05302	4.98304	6.16409	6.44971	7.01024	8.35397
		10	1.41661	2.55730	3.65679	4.36374	5.38706	6.68809	7.00295	7.62105	9.10380
2-1-1	10	0	1.05407	2.01847	2.92697	3.50032	4.31741	5.33780	5.58207	6.05894	7.19028
		1	1.61143	3.41955	5.03313	6.01962	7.39177	9.06000	9.45304	10.21417	11.99120
		2	1.74061	3.74227	5.53207	6.62817	8.15480	10.01355	10.45183	11.30091	13.28476
		10	1.88593	4.12760	6.15971	7.41546	9.17678	11.33780	11.84967	12.84353	15.17580
	20	0	1.16506	1.79827	2.37253	2.73785	3.26760	3.94770	4.11379	4.44177	5.23953
		1	1.36762	2.41057	3.41924	4.07131	5.02036	6.23561	6.53111	7.11275	8.51598
		2	1.42315	2.56202	3.66975	4.38734	5.43320	6.77442	7.10084	7.74365	9.29599
		10	1.49007	2.73447	3.95517	4.74993	5.91324	7.41307	7.77936	8.50208	10.25463
1-1-2	10	0	1.05407	2.01847	2.92697	3.50032	4.31741	5.33780	5.58207	6.05894	7.19028
		1	1.59772	3.40140	5.01917	6.01135	7.39476	9.08117	9.47911	10.25034	12.05370
		2	1.71767	3.70742	5.49821	6.59938	8.13792	10.01764	10.46176	11.32305	13.33941
		10	1.84829	4.06190	6.08325	7.33820	9.10487	11.28141	11.79822	12.80296	15.16665
	20	0	1.16506	1.79827	2.37253	2.73785	3.26760	3.94770	4.11379	4.44177	5.23953
		1	1.35422	2.38800	3.38972	4.03827	4.98350	6.19601	6.49118	7.07255	8.47710
		2	1.40319	2.52635	3.62140	4.33214	5.36984	6.70360	7.02869	7.66942	9.21950
		10	1.45993	2.67840	3.87668	4.65847	5.80500	7.28685	7.64935	8.36526	10.10477
2-2-1	10	0	1.05407	2.01847	2.92697	3.50032	4.31741	5.33780	5.58207	6.05894	7.19028
		1	1.54121	3.23199	4.73032	5.64224	6.90635	8.43768	8.79772	9.49424	11.11738
		2	1.65706	3.51279	5.15268	6.14955	7.53030	9.20148	9.59419	10.35375	12.12288
		10	1.79386	3.86524	5.71111	6.83940	8.40866	10.31638	10.76581	11.63610	13.66777
	20	0	1.16506	1.79827	2.37253	2.73785	3.26760	3.94770	4.11379	4.44177	5.23953
		1	1.33839	2.33014	3.28348	3.89780	4.78964	5.92820	6.20452	6.74784	8.05574
		2	1.38685	2.46532	3.50673	4.17838	5.15362	6.39856	6.70064	7.29457	8.72389
		10	1.44672	2.62590	3.77320	4.51601	5.59790	6.98406	7.32121	7.98491	9.58647
1-2-2	10	0	1.05407	2.01847	2.92697	3.50032	4.31741	5.33780	5.58207	6.05894	7.19028
		1	1.53203	3.22082	4.72285	5.63909	6.91140	8.45557	8.81903	9.52256	11.16377
		2	1.64085	3.49025	5.13347	6.13570	7.52736	9.21634	9.61387	10.38333	12.17824
		10	1.76608	3.82151	5.66652	6.79937	8.38043	10.30978	10.76531	11.64839	13.71436
	20	0	1.16506	1.79827	2.37253	2.73785	3.26760	3.94770	4.11379	4.44177	5.23953
		1	1.32848	2.31429	3.26329	3.87551	4.76521	5.90248	6.17873	6.72215	8.03163
		2	1.37186	2.43931	3.47222	4.13949	5.10983	6.35086	6.65238	7.24559	8.67534
		10	1.42370	2.58360	3.71513	4.44930	5.52072	6.89691	7.23219	7.89283	9.49015

foundations. The effects of the shear component of the foundations K_s are stronger than the effects of the Winkler component K_w.

The distribution of the normal stresses and transverse shear stresses through the thickness of the bi-FGSW plates are plotted in Fig. 8. According to this figure, the elastic foundations have significant effects on the distribution of the stresses of the bi-FGSW plate. When the plates lie on the elastic foundations, the maximum values of the stresses smaller than those of the plates without elastic foundations but the shapes of the distributions are almost unaffected.

Table 16. The dimensionless first nine frequencies ω^* of the square bi-FGSW platesof type B resting on elastic foundations.

Scheme	a/h	k	(1,1)	(1,2)	(2,2)	(1,3)	(2,3)	(1,4)	(3,3)	(2,4)	(3,4)
1-1-1	10	0	2.01559	4.52869	6.87076	8.34546	10.44555	13.06751	13.69520	14.92066	17.82853
		1	1.49793	3.28558	4.98677	6.07130	7.63131	9.60187	10.07706	11.00838	13.23585
		2	1.35869	2.94157	4.45861	5.42976	6.83142	8.60900	9.03873	9.88206	11.90470
		10	1.20373	2.55407	3.85825	4.69687	5.91164	7.45885	7.83391	8.57102	10.34438
	20	0	1.52845	2.87012	4.20295	5.07815	6.36912	8.05002	8.46325	9.28161	11.28217
		1	1.27496	2.23586	3.18337	3.80647	4.72826	5.93405	6.23148	6.82170	8.27108
		2	1.20923	2.06927	2.91161	3.46501	4.28385	5.35596	5.62065	6.14616	7.43831
		10	1.13316	1.88316	2.60897	3.08442	3.78737	4.70788	4.93525	5.38686	6.49849
1-2-1	10	0	2.01559	4.52869	6.87076	8.34546	10.44555	13.06751	13.69520	14.92066	17.82853
		1	1.59208	3.51393	5.33616	6.49538	8.15997	10.25838	10.76375	11.75354	14.11747
		2	1.47036	3.21553	4.88033	5.94320	7.47388	9.41006	9.87736	10.79362	12.98711
		10	1.32272	2.84947	4.31744	5.25904	6.62027	8.34991	8.76855	9.59067	11.56512
	20	0	1.52845	2.87012	4.20295	5.07815	6.36912	8.05002	8.46325	9.28161	11.28217
		1	1.32324	2.35203	3.36930	4.03843	5.02806	6.32183	6.64082	7.27360	8.82644
		2	1.26639	2.20617	3.13153	3.74004	4.64045	5.81883	6.10961	6.68674	8.10471
		10	1.19656	2.02983	2.84362	3.37803	4.16885	5.20473	5.46057	5.96865	7.21873
2-1-1	10	0	2.01559	4.52869	6.87076	8.34546	10.44555	13.06751	13.69520	14.92066	17.82853
		1	1.46208	3.21109	4.87186	5.92913	7.44816	9.36430	9.82596	10.73033	12.89128
		2	1.32674	2.88208	4.36737	5.31601	6.68252	8.41153	8.82890	9.64733	11.60701
		10	1.18100	2.52583	3.81640	4.64283	5.83571	7.34854	7.71425	8.43192	10.15303
	20	0	1.52845	2.87012	4.20295	5.07815	6.36912	8.05002	8.46325	9.28161	11.28217
		1	1.23595	2.17594	3.10334	3.71310	4.61486	5.79382	6.08453	6.66126	8.07680
		2	1.16528	2.00851	2.83592	3.37952	4.18358	5.23561	5.49520	6.01040	7.27620
		10	1.08466	1.82579	2.54664	3.01922	3.71779	4.63176	4.85732	5.30511	6.40591
1-1-2	10	0	2.01559	4.52869	6.87076	8.34546	10.44555	13.06751	13.69520	14.92066	17.82853
		1	1.47634	3.21825	4.87751	5.93566	7.45809	9.38168	9.84562	10.75495	12.93025
		2	1.33023	2.84981	4.30735	5.24050	6.58732	8.29532	8.70822	9.51853	11.46201
		10	1.18086	2.46663	3.70539	4.50019	5.64925	7.10931	7.46271	8.15673	9.82373
	20	0	1.52845	2.87012	4.20295	5.07815	6.36912	8.05002	8.46325	9.28161	11.28217
		1	1.28024	2.22219	3.14815	3.75659	4.65639	5.83318	6.12345	6.69942	8.11382
		2	1.21601	2.05187	2.86565	3.39930	4.18819	5.22032	5.47505	5.98071	7.22374
		10	1.14592	1.87618	2.57617	3.03297	3.70675	4.58698	4.80412	5.23509	6.29446
2-2-1	10	0	2.01559	4.52869	6.87076	8.34546	10.44555	13.06751	13.69520	14.92066	17.82853
		1	1.53735	3.39134	5.14816	6.26530	7.86892	9.88968	10.37624	11.32907	13.60421
		2	1.41236	3.08859	4.68557	5.70427	7.17030	9.02317	9.47014	10.34629	12.44263
		10	1.26968	2.74108	4.15141	5.05417	6.35698	8.00896	8.40827	9.19189	11.07107
	20	0	1.52845	2.87012	4.20295	5.07815	6.36912	8.05002	8.46325	9.28161	11.28217
		1	1.27855	2.27185	3.25376	3.89951	4.85440	6.10249	6.41017	7.02048	8.51788
		2	1.21437	2.11764	3.00701	3.59172	4.45670	5.58828	5.86744	6.42143	7.78208
		10	1.13830	1.94037	2.72472	3.23975	4.00163	4.99896	5.24515	5.73392	6.93561
1-2-2	10	0	2.01559	4.52869	6.87076	8.34546	10.44555	13.06751	13.69520	14.92066	17.82853
		1	1.54629	3.39168	5.14656	6.26476	7.87256	9.90247	10.39182	11.35072	13.64333
		2	1.41072	3.05233	4.62423	5.62986	7.08047	8.91891	9.36316	10.23481	12.32438
		10	1.25699	2.66070	4.01465	4.88441	6.14322	7.74489	8.13290	8.89522	10.72794
	20	0	1.52845	2.87012	4.20295	5.07815	6.36912	8.05002	8.46325	9.28161	11.28217
		1	1.31478	2.30709	3.28555	3.92892	4.88056	6.12516	6.43213	7.04121	8.53662
		2	1.25611	2.14907	3.02337	3.59761	4.44711	5.55903	5.83348	6.37833	7.71767
		10	1.18785	1.97036	2.72658	3.22161	3.95314	4.91050	5.14688	5.61628	6.77120

### 3.2.2. Free vibration analysis of bi-FGSW plate

Subsequently, the free vibration of the bi-FGSW plates is scrutinized in this section. The dimensionless first six frequencies of square bi-FGSW plates of type A and type B are presented in Table 15 and 16, respectively. Two parameters of the elastic foundations are $K_w = 100, K_s = 10$. The dimensionless of the frequency of the bi-FGSW plate of type A increases as increasing of the power-law index while the frequency of the bi-FGSW plate of type B decreases when the power-law index increases. Because when the power-law index increases, the effective Young's modulus of the bi-FGSW plates of type A increases while the effective mass density decreases. On the other hand, the effective Young's modulus decreases and the effective mass density increases

Table 17. The dimensionless fundamental frequencies ω^* of the square bi-FGSW platesof type A resting on elastic foundations.

Scheme	k	K_w, K_s								
		0,0	0,5	0,10	50,0	50,5	50,10	100,0	100,5	100,10
1-0-1	0	0.71641	0.84361	0.95398	0.78344	0.90122	1.00527	0.84516	0.95535	1.05407
	0.5	1.31840	1.39725	1.47187	1.35892	1.43554	1.50827	1.39826	1.47283	1.54380
	1	1.51128	1.58324	1.65206	1.54815	1.61847	1.68585	1.58417	1.65295	1.71898
	2	1.66135	1.72971	1.79547	1.69633	1.76334	1.82788	1.73060	1.79633	1.85973
	10	1.80273	1.86981	1.93457	1.83702	1.90289	1.96656	1.87068	1.93541	1.99803
1-1-1	0	0.71641	0.84361	0.95398	0.78344	0.90122	1.00527	0.84516	0.95535	1.05407
	0.5	1.20594	1.28965	1.36824	1.24905	1.33005	1.40638	1.29072	1.36925	1.44351
	1	1.36967	1.44582	1.51815	1.40877	1.48291	1.55351	1.44680	1.51909	1.58808
	2	1.50480	1.57622	1.64455	1.54140	1.61120	1.67810	1.57715	1.64543	1.71099
	10	1.65458	1.72230	1.78745	1.68923	1.75561	1.81956	1.72317	1.78829	1.85112
1-2-1	0	0.71641	0.84361	0.95398	0.78344	0.90122	1.00527	0.84516	0.95535	1.05407
	0.5	1.13130	1.21908	1.30094	1.17659	1.26122	1.34050	1.22020	1.30199	1.37893
	1	1.27367	1.35375	1.42934	1.31485	1.39256	1.46615	1.35478	1.43032	1.50206
	2	1.39279	1.46780	1.53915	1.43128	1.50437	1.57406	1.46877	1.54007	1.60822
	10	1.53243	1.60284	1.67027	1.56849	1.63735	1.70342	1.60375	1.67115	1.73593
2-1-1	0	0.71641	0.84361	0.95398	0.78344	0.90122	1.00527	0.84516	0.95535	1.05407
	0.5	1.22173	1.30539	1.38401	1.26481	1.34579	1.42217	1.30646	1.38502	1.45934
	1	1.39235	1.46869	1.54125	1.43153	1.50588	1.57673	1.46967	1.54218	1.61143
	2	1.53282	1.60477	1.67362	1.56969	1.64001	1.70744	1.60570	1.67451	1.74061
	10	1.68587	1.75480	1.82112	1.72114	1.78870	1.85381	1.75569	1.82198	1.88593
2-2-1	0	0.71641	0.84361	0.95398	0.78344	0.90122	1.00527	0.84516	0.95535	1.05407
	0.5	1.16215	1.24877	1.32975	1.20681	1.29043	1.36894	1.24987	1.33079	1.40705
	1	1.31515	1.39425	1.46909	1.35580	1.43265	1.50558	1.39526	1.47005	1.54121
	2	1.44327	1.51757	1.58839	1.48138	1.55385	1.62309	1.51853	1.58930	1.65706
	10	1.59033	1.66065	1.72810	1.62633	1.69515	1.76129	1.66156	1.72897	1.79386

Table 18. The dimensionless fundamental frequencies ω^* of the square bi-FGSW platesof type B resting on elastic foundations.

| Scheme	k	K_w, K_s								
		0,0	0,5	0,10	50,0	50,5	50,10	100,0	100,5	100,10
1-0-1	0	1.83005	1.89364	1.95516	1.86253	1.92505	1.98560	1.89447	1.95596	2.01559
	0.5	1.34578	1.41605	1.48299	1.38183	1.45035	1.51577	1.41695	1.48385	1.54786
	1	1.14556	1.22082	1.29171	1.18429	1.25723	1.32617	1.22179	1.29262	1.35976
	2	0.98077	1.06139	1.13631	1.02241	1.09998	1.17243	1.06242	1.13726	1.20747
	10	0.82708	0.91243	0.99045	0.87136	0.95275	1.02771	0.91350	0.99144	1.06367
1-1-1	0	1.83005	1.89364	1.95516	1.86253	1.92505	1.98560	1.89447	1.95596	2.01559
	0.5	1.45607	1.52530	1.59152	1.49155	1.55920	1.62403	1.52619	1.59237	1.65591
	1	1.28811	1.36133	1.43081	1.32571	1.39697	1.46475	1.36228	1.43171	1.49793
	2	1.13774	1.21553	1.28863	1.17779	1.25310	1.32412	1.21652	1.28957	1.35869
	10	0.96901	1.05273	1.13026	1.01229	1.09270	1.16757	1.05379	1.13125	1.20373
1-2-1	0	1.83005	1.89364	1.95516	1.86253	1.92505	1.98560	1.89447	1.95596	2.01559
	0.5	1.52744	1.59570	1.66116	1.56240	1.62920	1.69336	1.59659	1.66201	1.72496
	1	1.38661	1.45802	1.52609	1.42324	1.49289	1.55944	1.45894	1.52697	1.59208
	2	1.25596	1.33095	1.40193	1.29450	1.36737	1.43655	1.33192	1.40285	1.47036
	10	1.09582	1.17599	1.25103	1.13714	1.21459	1.28738	1.17701	1.25199	1.32272
2-1-1	0	1.83005	1.89364	1.95516	1.86253	1.92505	1.98560	1.89447	1.95596	2.01559
	0.5	1.42895	1.49604	1.56025	1.46332	1.52890	1.59179	1.49690	1.56108	1.62271
	1	1.26209	1.33180	1.39803	1.29787	1.36576	1.43042	1.33270	1.39889	1.46208
	2	1.12026	1.19276	1.26109	1.15756	1.22785	1.29433	1.19369	1.26197	1.32674
	10	0.96827	1.04369	1.11402	1.00719	1.07989	1.14800	1.04465	1.11492	1.18100
2-2-1	0	1.83005	1.89364	1.95516	1.86253	1.92505	1.98560	1.89447	1.95596	2.01559
	0.5	1.48719	1.55399	1.61803	1.52140	1.58676	1.64953	1.55485	1.61886	1.68044
	1	1.33858	1.40766	1.47351	1.37401	1.44140	1.50577	1.40855	1.47436	1.53735
	2	1.20767	1.27924	1.34701	1.24444	1.31401	1.38007	1.28016	1.34788	1.41236
	10	1.05824	1.13280	1.20274	1.09664	1.16876	1.23667	1.13375	1.20364	1.26968
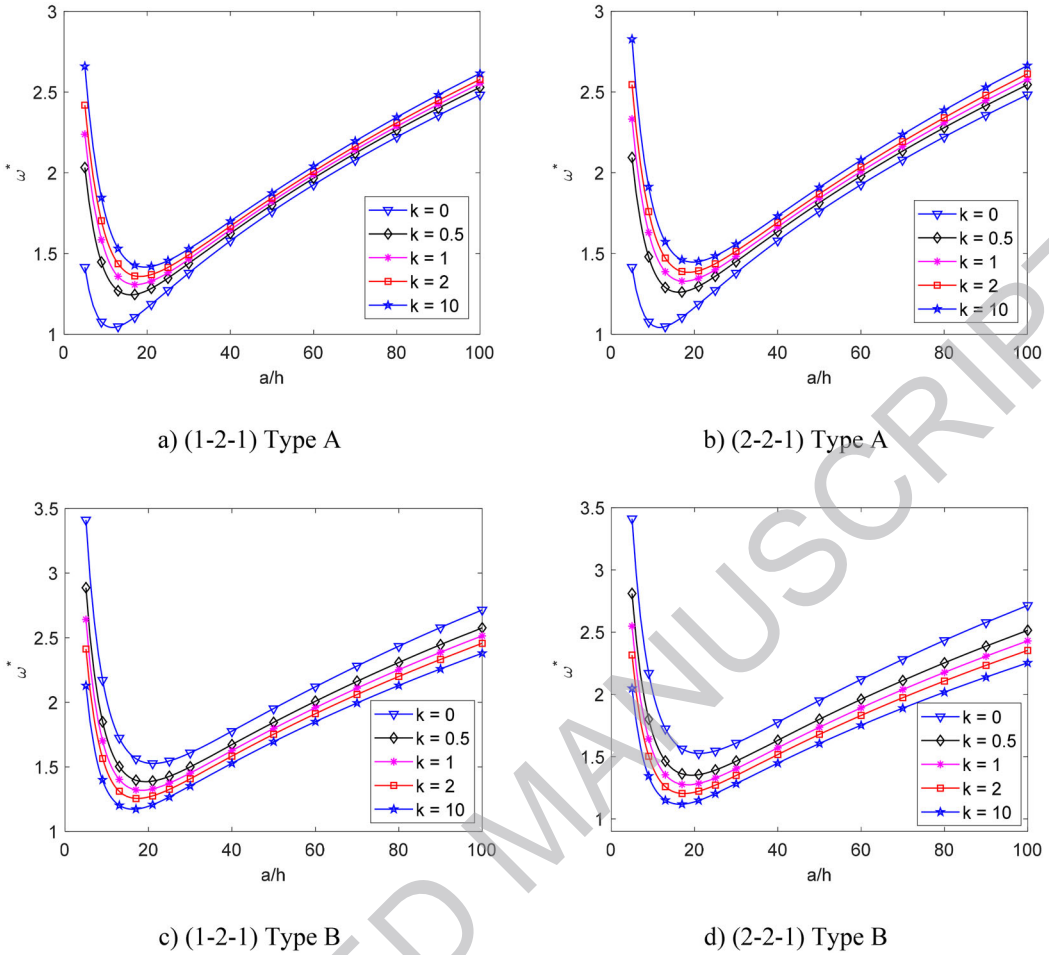
Figure 9. The variation of the dimensionless fundamental frequency ω^* of the square bi-FGSW plates as the function of side-to-thickness ratio.
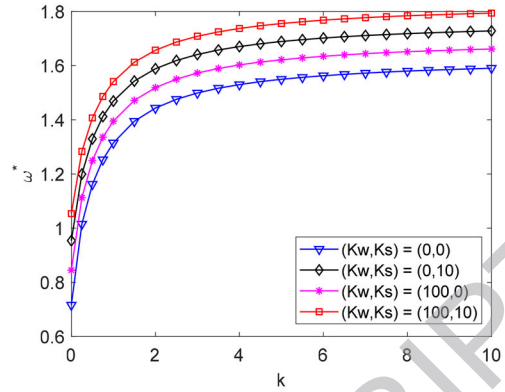
when the power-law index of the bi-FGSW plates of type B increases. So, it can be concluded that the material components have strong effects on the free vibration behavior of the bi-FGSW plates.

The dimensionless fundamental frequencies of the square bi-FGSW plate with the side-to-thickness ratio of $a/h = 10$ and the different values of the foundation parameters are presented in Tables 17 and 18. When the parameters of the elastic foundations raise, the frequencies of the bi-FGSW plates increase for all cases of the scheme of the sandwich plates.

Continuously, the effects of side-to-thickness ratio a/h on the fundamental frequency of the square bi-FGSW plates of type A and B with different values of the power-law index k are presented in Fig. 9. The side-to-thickness ratio change from 5 to 100 while the elastic foundation parameters are $K_w = 100, K_s = 10$. It can see clearly that when the side-to-thickness ratio is small, the increase of the side-to-thickness leads to the decrease of the frequency of the sandwich plates, then the frequency of the sandwich plates increases when the side-to-thickness ratio increase. The reason is that when the side-to-thickness ratio is small, the plate becomes a thick one, so the stiffness of the plate is much greater than the stiffness of the elastic foundations. Hence the increase of the side-to-thickness ratio leads to the decrease of the stiffness of the plate-elastic foundations system, so the frequency of the plate decreases. When the side-to-thickness ratio is high, the plate
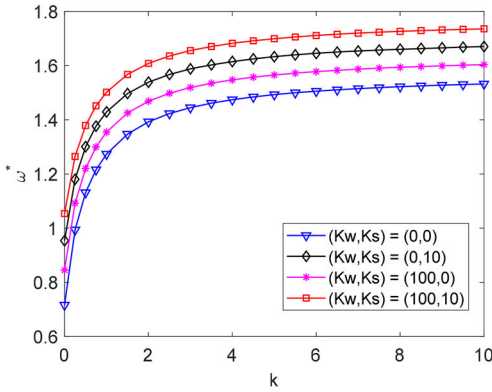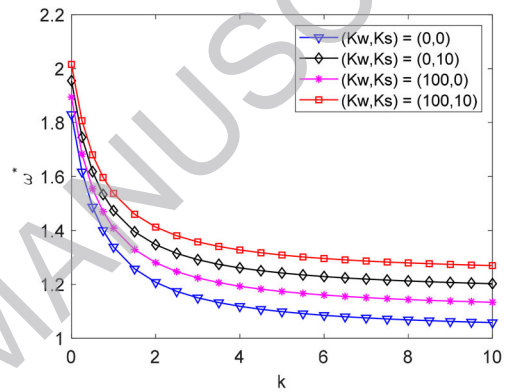
a) (1-2-1) Type A

b) (2-2-1) Type A
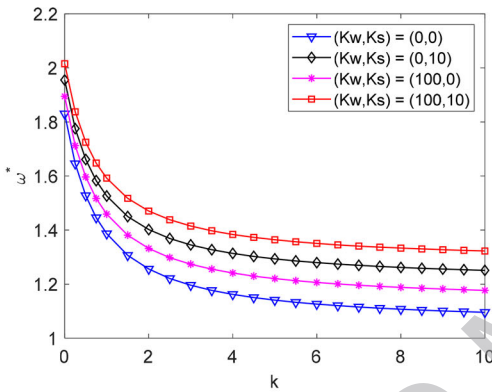
c) (1-2-1) Type B

d) (2-2-1) Type B

Figure 10. The variation of the dimensionless fundamental frequency ω^* of the square bi-FGSW plates as the function of power-law index.

becomes very thin one, the stiffness of the plate is much less than the stiffness of the elastic foundations. As a consequence, the stiffness of the coupled system of the plate and the elastic foundations is almost unchanged and approximates to the stiffness of the elastic foundations, but the inertia of the system decreases, hence the frequency of the plate increases. The minimum values of the frequencies depend on the values of the power-law index, the scheme and the type of the bi-FGSW plates. In cases of the bi-FGSW plate of type A, the value of the side-to-thickness ratio, where the minimum values of the frequency occur, increases when the power-law index increases. On the other hand, the value of the side-to-thickness ratio of the bi-FGSW plate of type B, where the minimum values of the frequency occur, decreases as the increase of the power-law index.

Continuously, the effects of the power-law index on the fundamental frequency of the square bi-FGSW plate of type A and type B with different values of elastic foundation parameters are presented in Fig. 10. It is obvious that when the power-law index increase, the frequency of the bi-FGSW plate of type A increase, but the frequency of the bi-FGSW plate of type B decrease. From Fig. 2, when the power-law index increases, the effective Young's modulus of the materials of two face sheets of the bi-FGSW plate of type A increases while the mass density of those decreases, so the frequency of such plate increases. On the other hand, when the power-law index increase, the effective Young's modulus of the materials of two face sheets of the bi-FGSW
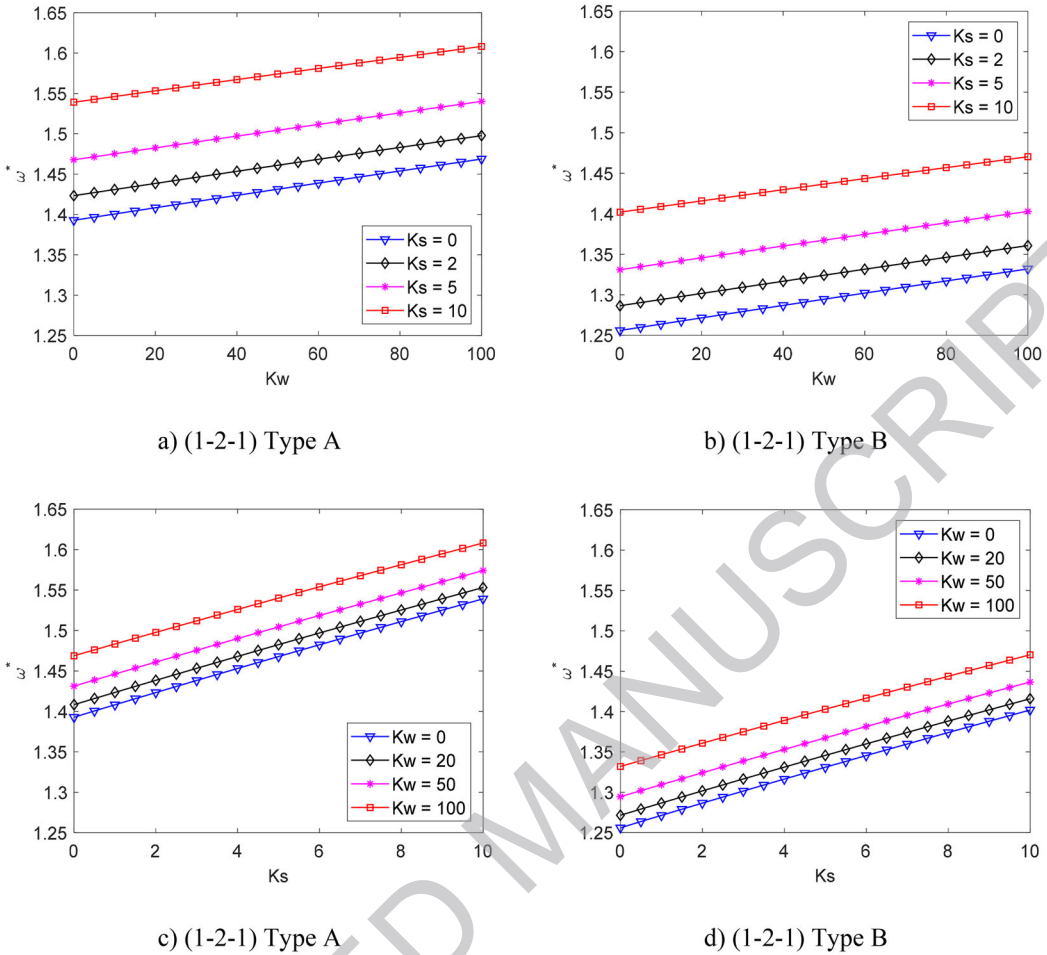
Figure 11. The effects of the elastic foundation parameters on the dimensionless fundamental frequency ω^* of the square bi-FGSW plates.

plate of type B decreases while the mass density of those increases, so the frequency of such plate decreases.

The effects of the elastic foundation parameters on the dimensionless fundamental frequency of square bi-FGSW plate are demonstrated in Fig. 11. From these figures, the frequency of the bi-FGSW plate of both types A and B increase as growing up of the elastic foundation's parameters. It is because when the stiffness of the elastic foundations increases, the stiffness of the system of plate-foundation increases. The effects of the shear layer are more significant than the Winkler spring layer of the elastic foundations.

4. Conclusions

In this work, a novel structure of the functionally graded sandwich plate with one homogeneous core and two different functionally graded face sheets have been investigated. A hybrid quasi-3D theory has been established and applied to study the deflections, stresses and free vibration behavior of the bi-FGSW plates resting on Pasternak's elastic foundations. The transverse shear strains and stresses are parabolical distribution through the thickness and equal to zero on two free surfaces of the plates, thus the proposed hybrid quasi-3D theory does not require any shear

correction factors. Based on the numerical results of the present work, some following remarkable conclusions can be achieved

- The static bending and free vibration behavior of the bi-FGSW plates are completely different in comparison with conventional FGSW plates, especially the distribution of the stresses through the thickness of the plates.
- When the power-law index increases, the deflections of the bi-FGSW plates of type A decrease, while the deflections of the bi-FGSW plates of type B increase.
- When the power-law index increases, the frequencies of the bi-FGSW plates of type A increase, but the frequencies of the bi-FGSW plates of type B decrease.
- The inclusion of the thickness stretching effects leads to the reduction of the results of the deflection and the enlargement of the results of the frequency of the plates.
- The deflections are decreased and the frequencies are increased with the inclusion of the elastic foundations.
- There is a minimum of the frequency of the bi-FGSW plates resting on elastic foundations when the ratio of side-to-thickness varies. This is a new point that has never been mentioned before.

Declaration of interests

No potential conflict of interest was reported by the author(s).

Funding

ORCID

Pham Van Vinh http://orcid.org/0000-0002-8053-6977

References

Abdelaziz, H. H., H. A. Atmane, I. Mechab, L. Boumia, A. Tounsi, and A. B. E. Abbas. 2011. Static analysis of functionally graded sandwich plates using an efficient and simple refined theory. *Chinese Journal of Aeronautics* 24 (4):434– 48. doi:10.1016/S1000-9361(11)60051-4.

Adhikari, B., and B. N. Singh. 2019. Dynamic response of functionally graded plates resting on two-parameter-based elastic foundation model using a quasi-3D theory. *Mechanics Based Design of Structures and Machines* 47 (4):399–429. doi:10.1080/15397734.2018.1555965.

Afshari, H., and N. Adab. 2020. Size-dependent buckling and vibration analyses of GNP reinforced microplates based on the quasi-3D sinusoidal shear deformation theory. *Mechanics Based Design of Structures and Machines*. doi:10.1080/15397734.2020.1713158.

Akavci, S. S. 2016. Mechanical behavior of functionally graded sandwich plates on elastic foundation. *Composites Part B: Engineering* 96 (1):136–52. doi:10.1016/j.compositesb.2016.04.035.

Altenbach, H., and V. A. Eremeyev. 2008. Direct approach-based analysis of plates composed of functionally graded materials. *Archive of Applied Mechanics* 78 (10):775–94. doi:10.1007/s00419-007-0192-3.

Arani, A. G., H. B. Zarei, and E. Haghparast. 2018. Vibration response of viscoelastic sandwich plate with magnetorheological fluid core and functionally graded-piezoelectric nanocomposite face sheet. *Journal of Vibration and Control* 24 (21):107754631774750. 5169-5185. doi:10.1177/1077546317747501.

Belalia, S. A. 2019. A new analysis of nonlinear free vibration behavior of bi-functionally graded sandwich plates using the p-version of the finite element method. *Mechanics of Advanced Materials and Structures* 26 (8): 727–40. doi:10.1080/15376494.2017.1410912.

Bennoun, M., M. S. A. Houari, and A. Tounsi. 2016. A novel five-variable refined plate theory for vibration analysis of functionally graded sandwich plates. *Mechanics of Advanced Materials and Structures* 23 (4):423–31. doi:10.1080/15376494.2014.984088.

Bessaim, A., M. S. Houari, A. Tounsi, S. Mahmoud, and E. A. A. Bedia. 2013. A new higher-order shear and normal deformation theory for the static and free vibration analysis of sandwich plates with functionally graded isotropic face sheets. *Journal of Sandwich Structures & Materials* 15 (6):671–703. doi:10.1177/1099636213498888.

Cheshmeh, E., M. Karbon, A. Eyvazian, D. W. Jung, M. Habibi, and M. Safarpour. 2020. Buckling and vibration analysis of FG-CNTRC plate subjected to thermo-mechanical load based on higher order shear deformation theory. *Mechanics Based Design of Structures and Machines*. doi:10.1080/15397734.2020.1744005.

Daikh, A. A., and A. Megueni. 2018. Thermal buckling analysis of functionally graded sandwich plates. *Journal of Thermal Stresses* 41 (2):139–5. doi:10.1080/01495739.2017.1393644.

Daikh, A. A., and A. M. Zenkour. 2019. Effect of porosity on the bending analysis of various functionally graded sandwich plates. *Materials Research Express* 6 (6):065703. doi:10.1088/2053-1591/ab0971.

Dorduncu, M. 2020. Stress analysis of sandwich plates with functionally graded cores using peridynamic differential operator and refined zigzag theory. *Thin-Walled Structures* 146:106468. doi:10.1016/j.tws.2019.106468.

Garg, A., H. D. Chalak, and A. Chakrabarti. 2020. Bending analysis of functionally graded sandwich plates using HOZT including transverse displacement effects. *Mechanics Based Design of Structures and Machines*. doi:10.1080/15397734.2020.1814157.

Gholamzadeh-Babaki, M. H., and M. Shakouri. 2019. Free and forced vibration of sandwich plates with electro-rheological core and functionally graded face layers. *Mechanics Based Design of Structures and Machines*. doi:10.1080/15397734.2019.1698436.

Iurlaro, L., M. Gherlone, and M. D. Sciuva. 2014. Bending and free vibration analysis of functionally graded sandwich plates using the Refined Zigzag Theory. *Journal of Sandwich Structures & Materials* 16 (6):669–99. doi:10.1177/1099636214548618.

Koizumi, M. 1997. FGM Activities in Japan. *Composites Part B: Engineering* 28 (1-2):1–4. doi:10.1016/S1359-8368(96)00016-9.

Li, Q., V. P. Iu, and K. P. Kou. 2008. Three-dimensional vibration analysis of functionally graded material sandwich plates. *Journal of Sound and Vibration* 311 (1-2):498–515. doi:10.1016/j.jsv.2007.09.018.

Liew, K. M., Z. X. Lei, and L. W. Zhang. 2015. Mechanical analysis of functionally graded carbon nanotube reinforced composites: A review. *Composite Structures* 120:90–7. doi:10.1016/j.compstruct.2014.09.041.

Liu, N., and A. E. Jeffers. 2017. Isogeometric analysis of laminated composite and functionally graded sandwich plates based on a layerwise displacement theory. *Composite Structures* 176 (15):143–53. doi:10.1016/j.compstruct.2017.05.037.

Mantari, J. L. 2015. Refined and generalized hybrid type quasi-3D shear deformation theory for the bending analysis of functionally graded shells. *Composites Part B: Engineering* 83:142–52. doi:10.1016/j.compositesb.2015.08.048.

Mantari, J. L., and E. V. Granados. 2015. A refined FSDT for the static analysis of functionally graded sandwich plates. *Thin-Walled Structures* 90:150–8. doi:10.1016/j.tws.2015.01.015.

Meiche, N. E., Tounsi, A. N. Ziane, I. Mechab, E., and A. A. Bedia. 2011. A new hyperbolic shear deformation theory for buckling and vibration of functionally graded sandwich plate. *International Journal of Mechanical Sciences* 53 (4):237–47. doi:10.1016/j.ijmecsci.2011.01.004.

Meziane, M. A. A., H. H. Abdelaziz, and A. Tounsi. 2014. An efficient and simple refined theory for buckling and free vibration of exponentially graded sandwich plates under various boundary conditions. *Journal of Sandwich Structures & Materials* 16 (3):293–318. doi:10.1177/1099636214526852.

Mohammadimehr, M.,. H. B. Zarei, A. Parakandeh, and A. G. Arani. 2017. Vibration analysis of double-bonded sandwich microplates with nanocomposite facesheets reinforced by symmetric and un-symmetric distributions of nanotubes under multi physical fields. *Structural Engineering and Mechanics* 64 (3):361–79. doi:10.12989/SEM.2017.64.3.361.

Mohseni, E., A. R. Saidi, and M. Mohammadi. 2017. Bending-stretching analysis of thick functionally graded micro-plates using higher-order shear and normal deformable plate theory. *Mechanics of Advanced Materials and Structures* 24 (14):1221–30. doi:10.1080/15376494.2016.1227503.

Natarajan, S., and G. Manickam. 2012. Bending and vibration of functionally graded material sandwich plates using an accurate theory. *Finite Elements in Analysis and Design* 57:32–42. doi:10.1016/j.finel.2012.03.006.

Neves, A. M. A., A. J. M. Ferreira, E. Carrera, M. Cinefra, R. M. N. Jorge, and C. M. M. Soares. 2012a. Buckling analysis of sandwich plates with functionally graded skins using a new quasi-3D hyperbolic sine shear deformation theory and collocation with radial basis functions. *ZAMM - Journal of Applied Mathematics and Mechanics / Zeitschrift Für Angewandte Mathematik Und Mechanik* 92 (9):749–66. doi:10.1002/zamm.201100186.

Neves, A. M. A., A. J. M. Ferreira, E. Carrera, M. Cinefra, R. M. N. Jorge, and C. M. M. Soares. 2012b. Static analysis of functionally graded sandwich plates according to a hyperbolic theory considering Zig-Zag and warping effects. *Advances in Engineering Software* 52:30–43. doi:10.1016/j.advengsoft.2012.05.005.

Neves, A. M. A., A. J. M. Ferreira, E. Carrera, M. Cinefra, R. M. N. Jorge, C. M. M. Soares, and A. L. Araujo. 2017. Influence of zig-zag and warping effects on buckling of functionally graded sandwich plates according to sinusoidal shear deformation theories. *Mechanics of Advanced Materials and Structures* 24 (5):360–76. 43. doi:10.1080/15376494.2016.1191095.

Neves, A. M. A., A. J. M. Ferreira, E. Carrera, M. Cinefra, C. M. C. Roque, R. M. N. Jorge, and C. M. M. Soares. 2013. Static, free vibration and buckling analysis of isotropic and sandwich functionally graded plates using a quasi-3D higher-order shear deformation theory and a meshless technique. *Composites Part B: Engineering* 44 (1):657–74. doi:10.1016/j.compositesb.2012.01.089.

Nguyen, H. N., T. T. Hong, P. V. Vinh, N. D. Quang, and D. V. Thom. 2019. A refined simple first-order shear deformation theory for static bending and free vibration analysis of advanced composite plates. *Materials* 12 (15):2385. doi:10.3390/ma12152385.

Nguyen, V. H., T. K. Nguyen, H. T. Thai, and T. P. Vo. 2014. A new inverse trigonometric shear deformation theory for isotropic and functionally graded sandwich plates. *Composites Part B: Engineering* 66:233–46. doi:10.1016/j.compositesb.2014.05.012.

Nguyen, T. K., T. P. Vo, and H. T. Thai. 2014. Vibration and buckling analysis of functionally graded sandwich plates with improved transverse shear stiffness based on the first-order shear deformation theory. *Proceedings of the Institution of Mechanical Engineers, Part C: Journal of Mechanical Engineering Science* 228 (12):2110–31. doi:10.1177/0954406213516088.

Pandey, S., and S. Pradyumna. 2015. Free vibration of functionally graded sandwich plates in thermal environment using a layerwise theory. *European Journal of Mechanics - A/Solids* 51:55–66. doi:10.1016/j.euromechsol.2014.12.001.

Pandya, B. N., and T. Kant. 1988. Higher-order shear deformable theories for flexure of sandwich plates-Finite element evaluations. *International Journal of Solids and Structures* 24 (12):1267–86. doi:10.1016/0020-7683(88)90090-X.

Pham, V. V., T. D. Nguyen, C. T. Nguyen, V. T. Do, and K. H. Le. 2020. Modified single variable shear deformation plate theory for free vibration analysis of rectangular FGM plates. *Structures* 29:1435–44. doi:10.1016/j.istruc.2020.12.027.

Reddy, J. N. 1984. A simple higher-order theory for laminated composite plates. *Journal of Applied Mechanics* 51 (4):745–52. doi:10.1115/1.3167719.

Reddy, J. N. 2000. Analysis of functionally graded plates. *International Journal for Numerical Methods in Engineering* 47 (1-3):663–84. doi:10.1002/(SICI)1097-0207(20000110/30)47:1/3 < 663::AID-NME787 > 3.0.CO;2-8.

Sobhy, M. 2013. Buckling and free vibration of exponentially graded sandwich plates resting on elastic foundations under various boundary conditions. *Composite Structures* 99:76–87. doi:10.1016/j.compstruct.2012.11.018.

Swaminathan, K., D. T. Naveenkumar, A. M. Zenkour, and E. Carrera. 2015. Stress, vibration and buckling analyses of FGM plates - A state-of-the-art review. *Composite Structures* 120:10–31. doi:10.1016/j.compstruct.2014.09.070.

Taibi, F. Z., S. Benyoucef, A. Tounsi, R. B. Bouiadjra, E. A. A. Bedia, and S. R. Mahmoud. 2015. A simple shear deformation theory for thermo-mechanical behaviour of functionally graded sandwich plates on elastic foundations. *Journal of Sandwich Structures & Materials* 17 (2):99–129. doi:10.1177/1099636214554904.

Thai, H. T., and S. E. Kim. 2015. A review of theories for the modeling and analysis of functionally graded plates and shells. *Composite Structures* 128 (15):70–86. doi:10.1016/j.compstruct.2015.03.010.

Thai, H. T., T. K. Nguyen, T. P. Vo, and J. Lee. 2014. Analysis of functionally graded sandwich plates using a new first-order shear deformation theory. *European Journal of Mechanics - A/Solids* 45:211–25. doi:10.1016/j.euromechsol.2013.12.008.

Van, T. D., V. P. Van, and N. N. Hoang. 2020. On the development of refined plate theory for static bending behavior of functionally graded plates. *Mathematical Problems in Engineering* 2020:2836763. doi:10.1155/2020/2836763.

Vu, T. V., N. V. Hieu, C. H. Nguyen, T. P. Nguyen, and J. L. Curiel-Sosa. 2021. Meshfree analysis of functionally graded plates with a novel four-unknown arctangent exponential shear deformation theory. *Mechanics Based Design of Structures and Machines.* doi:10.1080/15397734.2020.1863227.

Xiang, S., and Y. Q. Liu. 2016. An *n*th-order shear deformation theory for static analysis of functionally graded sandwich plates. *Journal of Sandwich Structures & Materials* 18 (5):579–96. doi:10.1177/1099636216647928.

Zenkour, A. M. 2005a. A comprehensive analysis of functionally graded sandwich plates: Part 1 Deflection and stresses. *International Journal of Solids and Structures* 42 (18-19):5224–42. doi:10.1016/j.ijsolstr.2005.02.015.

Zenkour, A. M. 2005b. A comprehensive analysis of functionally graded sandwich plates: Part 2 - Buckling and free vibration. *International Journal of Solids and Structures* 42 (18-19):5243–58. doi:10.1016/j.ijsolstr.2005.02.016.

Zenkour, A. M. 2013. Bending analysis of functionally graded sandwich plates using a simple four-unknown shear and normal deformations theory. *Journal of Sandwich Structures & Materials* 15 (6):629–56. doi:10.1177/1099636213498886.

Zhang, L. W., Z. G. Song, and K. M. Liew. 2016. Optimal shape control of CNT reinforced functionally graded composite plates using piezoelectric patches. *Composites Part B: Engineering* 85:140–9. doi:10.1016/j.compositesb.2015.09.044.

Zhang, L. W., Y. Zhang, G. L. Zou, and K. M. Liew. 2016. Free vibration analysis of triangular CNT-reinforced composite plates subjected to in-plane stresses using FSDT element-free method. *Composite Structures* 149:247–60. doi:10.1016/j.compstruct.2016.04.019.